ON LARGE-SCALE HEATING

AND

ATMOSPHERIC WAVES

BY

A. WIIN-NIELSEN

EUROPEAN CENTRE FOR MEDIUM-RANGE WEATHER FORECASTS

On Large-Scale Heating and Atmospheric Waves

by

A.C. Wiin-Nielsen

European Centre for Medium Range Weather Forecasts

Abstract

The speed of propagation and the rate of damping are found for quasi-geostrophic, large-scale, atmospheric waves influenced by a Newtonian heating. Using perturbation theory on a basic state of rest, but characterized by stratification it is possible to derive the speed of propagation which to this approximation is uninfluenced by the heating and the damping rate as a function of the stratification, the wavelength and other parameters in the problem. It turns out that the shortest e-damping time is found for the largest scale of motion.

The energy conversion between available potential energy and kinetic energy as well as the generation of available potential energy are calculated from the perturbation solution. Each of these quantities turn out to be negative because of the nature of the Newtonian heating. The ratio of the two energy quantities is particularly simple and is easily calculated for each vertical model and stratification as a function of the wavelength. This calculation shows that the available potential energy will decrease regardless of the wavelength, but the rate of decrease is larger for increasing values of the wavelength.

A two level model is used to consider the effects of heating in the case of a non-zero basic flow with the result that the Newtonian heating will damp the solution which is analogous to the barotropic Rossby waves.

The last sections of the paper contain some results of tendency calculations of the geopotential, the surface pressure and the vertical velocity for given heating rates. The tendencies depend upon the thermal stratification, the vertical distribution of the heating and other parameters. In agreement with other investigations one can conclude that the heating has a significant, modifying influence on the atmospheric waves, in particular those of the largest scale.

1. Introduction

Several investigations of the influence of diabatic heating on cyclogenesis and on the development of atmospheric waves have been made. Döös (1961) investigated the scale of the heating as a factor in cyclogenesis and found that the pressure fall at the surface increases monotonically with increasing dimensions in the case where the maximum intensity is proportional to the horizontal dimension. A number of empirical investigations by Petterssen (1950, 1955) and Winston (1955) have clearly demonstrated that there is a marked tendency for new cyclones to form or existing ones to intensify over water bodies which are warm relative to the surroundings.

The influence of heating on the baroclinic waves has been investigated by Wiin-Nielsen et al (1967) in a simple, two level model with the result that there is a change in the region of instability, and that heating in general will alter the growth rate of baroclinically unstable waves. A similar result has been obtained by Haltiner (1967) who investigated the influence of the sensible heat exchange on the development of baroclinic waves with the result that the heating decreases the degree of instability for intermediate wavelengths but creates instability on the large scale.

The formulation of the heating function is in general a very complicated matter because the total heating depends upon a number of physical processes. However, as long as we restrict ourselves to

the large-scale, quasi-geostrophic motion and are willing to make the approximation of linearization it has been shown (Wiin-Nielsen, 1972) that the major heating processes in a two level model can be expressed in a Newtonian form in which the coefficient and the equilibrium temperature field depend upon the various processes under consideration. It is naturally realized that some processes such as evaporation and condensation are impossible to incorporate in such a simple formulation, but it is also true that they are most active outside the quasi-geostrophic regime. It is, in any case, of interest to analyse the influence of Newtonian heating on atmospheric waves realising that we must expect to limit the applicability of the results of such an analysis to the large-scale features of the atmosphere. An investigation of this kind was carried out by Fisher and Wiin-Nielsen (1971), but the analysis was restricted to an atmospheric model which applies to the ultra-long waves only. It was shown in that case that the only effect of the heating on the phase speed is the addition of a purely imaginary part to the phase speed for the adiabatic case indicating that the speed of propagation is unchanged and that the growth rate is reduced by the heating. In view of the fact that these results were obtained for a somewhat specialized model it is of interest to explore if these results can be obtained for the general, quasi-geostrophic model.

In the present investigation we shall first select a basic state which is characterized by no motion and by a given thermal stratification. This means that we do not have the possibility to investigate any

instabilities generated by horizontal or vertical shear. On the other hand, we have the advantage that the results will show the direct influence of the heating on the phase speed without the complications generated by other physical factors. We shall also consider the non-zero basic flow in the two level case.

2. The Perturbation Analysis

As mentioned in the introduction we shall employ Newtonian heating as the forcing function. This means that we shall assume that the heating is of the form

$$H = -C_p \gamma (T-T_E) \tag{2.1}$$

in which C_p is the specific heat for constant pressure, γ a constant, T the temperature and T_E the equilibrium temperature. When we take the zonal average of (2.1), indicated by a subscript Z, we obtain

$$H_Z = -C_p \gamma (T_Z-T_{EZ}) \tag{2.2}$$

We shall assume for simplicity that the equilibrium temperature T_E is a function of the latitude and pressure only from which it follows that $T_E = T_{EZ}$. Subtracting (2.2) from (2.1) we thus obtained

$$H' = -C_p \gamma T' \tag{2.3}$$

where the prime indicates a deviation from the zonal average. Using the gas equation and the hydrostatic equation we may also write (2.3) in the form

$$H' = \frac{C_p}{R} \gamma p \frac{\partial \Phi'}{\partial p} \tag{2.4}$$

in which R is the gas constant, p the pressure, and Φ' the perturbation geopotential.

The thermodynamic equation for the perturbations considering a basic state of rest is

$$\frac{\partial}{\partial t}\left(\frac{\partial \Phi}{\partial p}\right) + \bar{\sigma}\,\omega = -\frac{R}{C_p}\,\frac{1}{p}\,H \tag{2.5}$$

in which we have dropped the prime on the perturbation quantities and indicated the parameters referring to the basic state by a bar. Inserting (2.4) in (2.5) we get

$$\frac{\partial}{\partial t}\left(\frac{\partial \Phi}{\partial p}\right) + \bar{\sigma}\,\omega = -\,\gamma\,\frac{\partial \Phi}{\partial p} \tag{2.6}$$

The quantity $\bar{\sigma}$ in (2.5) and (2.6) is a measure of the static stability in the basic state. $\bar{\sigma}$ is in the quasi-geostrophic case a function of pressure only. The dependence of $\bar{\sigma}$ on pressure is of considerable importance for the nature of the solution to the eigenvalue problem to be considered later. The most simple assumption is naturally to consider $\bar{\sigma}$ to be a constant, and we shall use this assumption in order to obtain the most simple mathematical analysis. In many earlier investigations, see for example Wiin-Nielsen (1959) and Gates (1961), it has been assumed that $\bar{\sigma}$ is inversely proportional to a power of the pressure. Such an assumption describes the vertical variation of $\bar{\sigma}$ with a reasonable accuracy. Still another assumption which is frequently made is to assume a constant lapse rate atmosphere, see Jacobs and Wiin-Nielsen (1966). From the definition of $\bar{\sigma}$, i.e.

$$\bar{\sigma} = -\,\frac{\bar{\alpha}}{\bar{\Theta}}\,\frac{d\bar{\Theta}}{dp} \tag{2.7}$$

one obtains using the definition of potential temperature and the hydrostatic equation that

$$\bar{\sigma} = \frac{R^2}{g}\,\frac{\bar{T}}{p^2}\,(\gamma_d - \gamma) \tag{2.8}$$

in which g is the acceleration of gravity, $\gamma = -d\bar{T}/d_z = \text{const.}$ and $\gamma_d = g/C_p$ the dry-adiabatic lapse. In (2.8) $\bar{T}$ is strictly

a function of pressure, and we shall return to this point later, but it is evident that $\bar{T}$ varies much slower than p^2 with pressure. It is therefore a reasonable approximation to assume that

$$\bar{\sigma} = \frac{\sigma_o}{p_*^2} \tag{2.9}$$

in which $p_* = p/p_o$ is a nondimensional quantity, $p_o = 100cb$ is a standard value of the surface pressure and

$$\sigma_o = \frac{R^2 \bar{T}_s}{g p_o^2} (\gamma_d - \gamma) \tag{2.10}$$

in which $\bar{T}_s$ is a standard value of the temperature. Refining this assumption we note the well known result that the vertical variation of temperature in a constant lapse rate atmosphere is

$$\bar{T} = \bar{T}_o p_*^{\frac{R\gamma}{g}} \tag{2.11}$$

With this result we may write (2.8) in the form

$$\bar{\sigma} = \frac{\bar{\sigma}_o}{p_*^{2-\frac{R\gamma}{g}}} \tag{2.12}$$

with

$$\sigma_o = \frac{R^2 \bar{T}_o}{g p_o^2} (\gamma_d - \gamma) \tag{2.13}$$

In addition to (2.6) we will need the vorticity equation which, considering the basic state, may be written in the form

$$\frac{\partial \nabla^2 \Phi}{\partial t} + \beta \frac{\partial \Phi}{\partial x} = f_o^2 \frac{\partial \omega}{\partial p} \tag{2.14}$$

in which we have already introduced the geostrophic approximation for the vorticity, i.e. $\zeta \doteq f^{-1} \nabla^2 \Phi$.

Assuming perturbations of the form

$$\Phi = \Phi_*(p)e^{ik(x-ct)}$$
$$\omega = \Omega(p)e^{ik(x-ct)} \qquad (2.15)$$

and introducing (2.15) into (2.14) and (2.6) we get

$$ik(C+C_R)\Phi_* = C_I^2 \frac{d\Omega}{dp}$$
$$- ik(C+iC_H)\frac{d\Phi_*}{dp} + \bar{\sigma}\,\Omega = 0 \qquad (2.16)$$

where we have introduced the following notations

$$C_R = \frac{\beta}{k^2}$$
$$C_R = \frac{f_o}{k} \qquad (2.17)$$
$$C_H = \frac{\gamma}{k}$$

Eliminating Φ_* from the system (2.16) we find

$$\frac{d^2\Omega}{dp_*^2} - \frac{C_g^2}{C_I^2}\,\frac{C+C_R}{C+iC_H}\,\Omega = 0 \qquad (2.18)$$

in which

$$C_g = C_g(p) = p_o\,\bar{\sigma}^{\frac{1}{2}} \qquad (2.19)$$

(2.18) constitutes the eigenvalue problem which will have to be solved satisfying the boundary conditions

$$\Omega = 0 \quad \text{at } p_* = 0 \text{ and } p_* = 1 \qquad (2.20)$$

It is apparent from (2.18) that $C_g = C_g(p)$ determines the whole solution of the problem, and that the nature of $\Omega = \Omega(p)$ determines the degree of difficulty in the determination of the eigenvalue.

3. Solutions with $\bar{\sigma}$ = Const.

3.1 Adiabatic Case.

We shall first of all consider some elementary solutions which will serve the purpose of providing the background for other more complicated cases. The initial assumption on C_g is therefore C_g = const. Denoting

$$q_1^2 = -\frac{C_g^2}{C_I^2}\frac{C+CR}{C} \tag{3.1}$$

we consider first the adiabatic case ($C_H = 0$). The solution of (2.18) is

$$\Omega = C_1 \cos(q_1 p_*) + C_2 \sin(q_1 p_*) \tag{3.2}$$

The boundary condition at $p_* = 0$ gives $C_1 = 0$, while the condition at $p_* = 1$ requires

$$q_1 = m\pi \tag{3.3}$$

when m = 0, 1, 2, 3, ... Inserting (3.3) in (3.1) we find solving for C that

$$C = -\frac{C_R}{1+m^2\pi^2\frac{C_I^2}{C_g^2}} \tag{3.4}$$

We note from (3.4) that m = 0 gives the normal Rossby phase velocity while the other values of m give the phase speed of the higher vertical modes, which will retrograde with a speed considerably smaller than the pure Rossby mode.

3.2 Long Wave Approximation

As shown by Wiin-Nielsen (1961) it is possible to filter out the pure Rossby mode by neglecting the time derivative in the vorticity equation. This approximation is normally called the ultra long wave approximation because for the largest scale there is an approximative balance between the beta effect and the divergence effect. The implication of the assumption is that the quantity q^2 now takes the value

$$q_2^2 = -\frac{C_g^2}{C_I^2}\frac{C_R}{C} \tag{3.5}$$

while (3.2) and (3.3) still apply. We find therefore that

$$C = -\frac{C_R}{m^2\pi^2\frac{C_I^2}{C_g^2}} = -\frac{\beta}{m^2\pi^2\frac{f_o^2}{Cg^2}} \tag{3.6}$$

which comparing to (3.4) is identical to assuming

$$1 \ll m^2\pi^2\frac{C_I^2}{C_g^2} \tag{3.7}$$

The approximation is thus clearly valid only for very long waves.

The case treated above is adiabatic, but the long wave approximation can clearly also be made in the case of Newtonian heating. In that case we have

$$q_3^2 = -\frac{Cg^2}{C_I^2}\frac{C_R}{C+iC_H} \tag{3.8}$$

Using again (3.2) and (3.3) we find that

$$C = -\frac{\beta}{m^2\pi^2\frac{f_o^2}{C_g^2}} - iC_H \tag{3.9}$$

This result agrees with the more general result obtained by Fisher and Wiin-Nielsen (1971) using a model with vertical windshear that in a model applying to the ultralong waves the Newtonian heating will introduce a damping which is proportional to the wavelength because

$$C_H = \frac{\gamma}{k} = \frac{\gamma}{2\pi} L \tag{3.10}$$

where L is the wavelength. It should however be pointed out that the e-damping time is independent of the wavelength because

$$T_e = \frac{1}{kC_i} = \frac{1}{kC_H} = \frac{1}{\gamma} \tag{3.11}$$

3.3 The General Case.

In this case we have

$$q_4^2 = -\frac{C_g^2}{C_I^2} \qquad \frac{C+C_R}{C+iC_H} = a+ib \tag{3.12}$$

with the solution of (2.18)

$$\Omega = C_3 e^{iq_4 p_*} + C_4 e^{-iq_4 p_*} \tag{3.13}$$

The boundary condition at $p_*=0$ gives $C_3 = -C_4$ and

$$\Omega = C_3 \left(e^{iqp_4 *} - e^{-iqp_4 *}\right) \tag{3.14}$$

Assuming that $C = C_r + iC_i$ and $q_4 = q_r + iq_i$ we get after some elementary calculations

$$\Omega = \left\{-2\sinh(q_i p_*)\cos q_r p_* \; C_r - 2\cosh(q_i p_*)\sin q_r p_* \; C_i\right\} + i\left\{2\cosh(q_i p_*)\sin q_r p_* \; C_r - 2\sin h(q_i p_*)\cos q_r p_* \; C_i\right\} \tag{3.15}$$

For $p_*=1$ we must require that both the real and the imaginary part of Ω vanish leading to the equation

$$\sinh^2 q_i \cos^2 q_r + \cosh^2 q_i \sin^2 q_r = 0 \tag{3.16}$$

(3.16) is satisfied only if each of the two terms is zero. Since $\cosh^2 q_i \neq 0$, we must require that $\sin^2 q_r = 0$, leading to

$$q_r = m\pi \tag{3.17}$$

With this value of q_r for which $\cos^2 q_r \neq 0$, we must require $\sinh^2 q_i = 0$ which means

$$q_i = 0 \tag{3.18}$$

The remaining calculations are required to determine q_r and q_i. Using (3.12) we find

$$\begin{aligned} q_r &= \left(\frac{A+a}{2}\right)^{\frac{1}{2}} \\ q_i &= \left(\frac{A-a}{2}\right)^{\frac{1}{2}} \end{aligned} \tag{3.19}$$

where

$$A = (a^2+b^2)^{\frac{1}{2}}$$

In order to satisfy (3.18) it is required that A = a or b = 0. From this it follows that

$$q_r^2 = a = m^2\pi^2 \tag{3.21}$$

Returning again to (3.12) we find the following conditions

$$a = -\frac{C_g^2}{C_I^2} \frac{C_r(C_r+C_R) + C_i(C_i+C_H)}{C_r^2 + (C_i+C_H)^2} = m^2\pi^2 \tag{3.22}$$

$$b = \frac{C_g^2}{C_I^2} \frac{C_H C_r + C_R C_i + C_R C_H}{C_r^2 + (C_i+C_H)^2} = 0 \tag{3.23}$$

which must be solved for C_r and C_i. The solution can again be obtained by elementary methods because we have a coupled system of a first and a second degree equation. The solutions are

$$C_r = 0 \text{ and } C_r = -\frac{C_R}{1+Q} \tag{3.24}$$

and

$$C_i = -C_H \text{ and } C_i = \frac{-Q}{1+Q} CH \tag{3.25}$$

where

$$Q = m^2\pi^2 \frac{C_I^2}{C_g^2} \tag{3.26}$$

We notice first of all that C_r, apart from the trivial solution $C_r = 0$, is unchanged compared to the adiabatic case (see eq.(3.4)), while the imaginary part shows that the Newtonian heating will act as a damping effect, but in a more complicated way than in the ultra-long wave case (see eq. (3.9)). We remark, however, that C_i in (3.25) will approach $-C_H$ when the wavelength increases toward infinity.

The main results of this section are summarized in Fig.1 and Fig.2 of which the first shows the real part of the phase speed for the first three vertical modes (m = 1, 2, 3) as a function of wavelength together with the three asymptotic values, marked A_S . It is seen that the higher modes move slowly from east to west and that they approach their asymptotic values at rather small values of the wavelength. On the other hand, the lowest vertical modes move more rapidly from east to west and approach the asymptotic value more slowly. Fig.2 shows that the higher modes are damped more rapidly

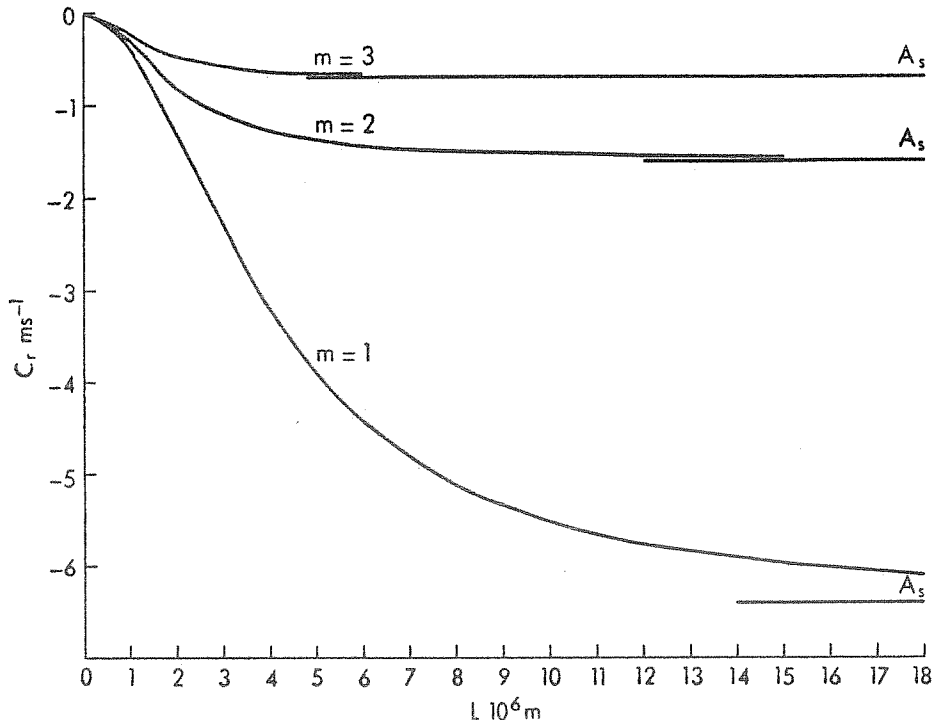

Fig.1: Real part of the phase speed in the case of constant stability ($\bar{\sigma}$ = 4). Horizontal lines marked A_s show the asymptotic values for very large scales.

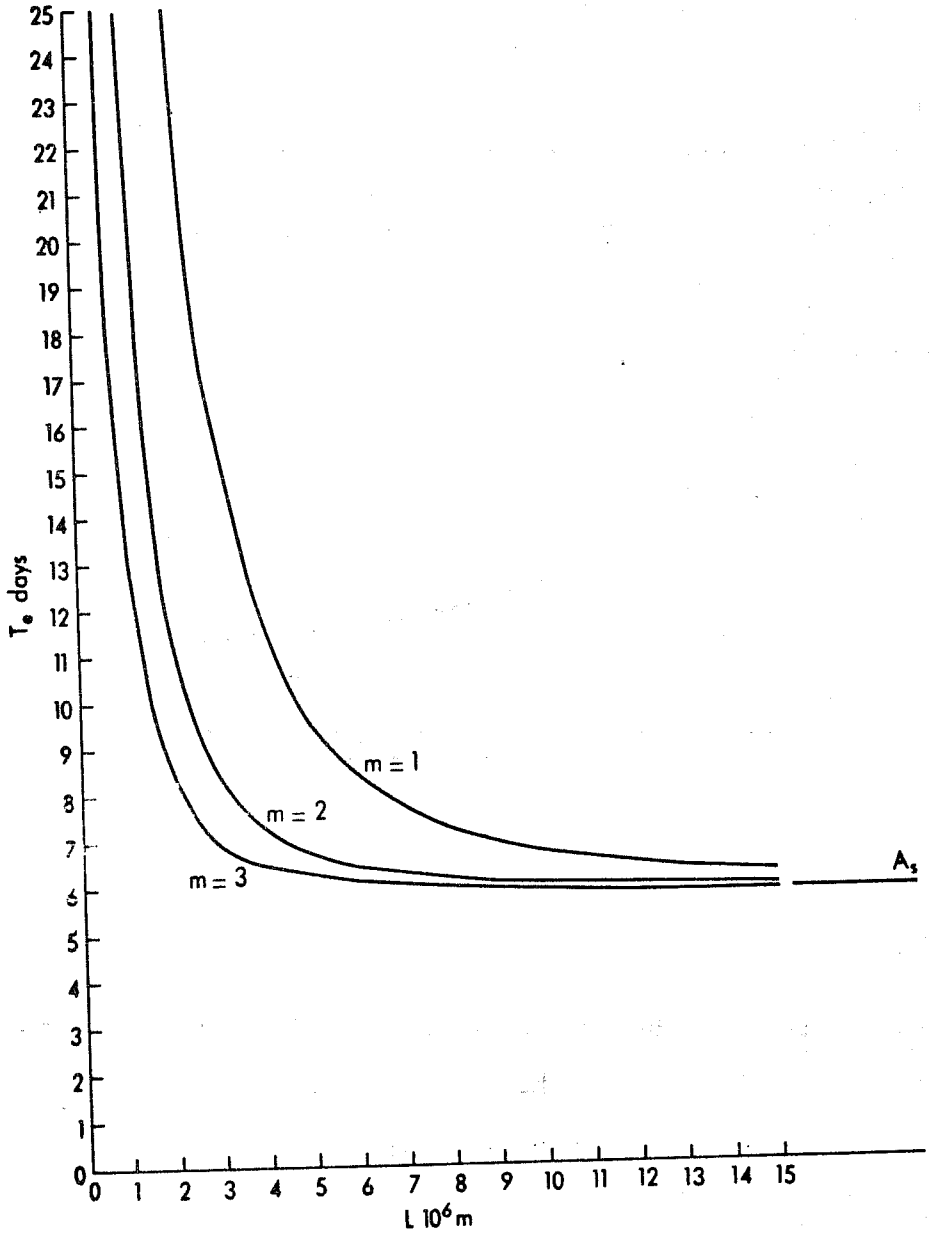

Fig.2: The e-damping time in days as a function of wavelength, measured in 10^6m. Same parameters as in fig.1.

than the lower vertical mode. It is also evident that the short waves are only weakly damped with large values of T_e . The asymptotic damping time for large values of the wavelength is of the order of six days and is approached more rapidly for the higher modes.

The analysis in this section in which the static stability parameter has been assumed constant is needless to say very simple from a mathematical point of view. In the next section we shall treat a more realistic stratification in which $\bar{\sigma}$ varies with the pressure. It is naturally also possible to use the results of the perturbation analysis to calculate the energetics of the waves. Such an analysis will be made at the end of the next section.

4. The Constant Lapse Rate Case.

The problem in this section is to solve (2.18) where $\bar{\sigma}$ is given by (2.12) and (2.13). Equations (2.18) can in this case be written in the form

$$p_*^2 \frac{d^2\Omega}{dp_*^2} + q_5^2 p_*^m \Omega = 0 \tag{4.1}$$

where

$$m = \frac{R\gamma}{g} \tag{4.2}$$

and

$$q_5^2 = - \frac{\sigma_o p_o^2}{C_I^2} \frac{C+C_R}{C+iC_H} \tag{4.3}$$

in which

$$\sigma_o = \frac{R^2 T_o}{g p_o^2} (\gamma_d - \gamma) \tag{4.4}$$

The solution to (4.1) satisfying the condition $\Omega = 0$ at $p_* = 0$ is

$$\Omega = C_5\, p_*^{\frac{1}{2}}\, J_n(2nq_5 p_*^{\frac{1}{2n}}),\quad n = \frac{1}{m} > 0 \tag{4.5}$$

We must next satisfy the condition that $\Omega = 0$ at $p_* = 1$. It is known that all zeroes of the Bessel function for $n > -1$ are real. It follows therefore that the imaginary part of q_5 is zero because q must satisfy the relation

$$J_n(2nq_5) = 0 \tag{4.6}$$

Denoting an analogy with section 3 $q_5 = q_r + iq_i$ we know that $q_i = 0$, and that q_r can take all values determined by $2nq_r = j$ where j is an arbitrary zero of the Bessel function. Using again the results and notations introduced by (3.12), (3.19) and (3.20) we find the following equations for the determination of C_r and C_i

$$C_H C_r + C_R C_i = -C_R C_H \tag{4.7}$$

$$\frac{C_r(C_r+C_R)+C_i(C_i+C_H)}{C_r^2+(C_i+C_H)^2} = -\frac{C_I^2}{\sigma_o p_o^2}\; q_r^2 = -Q_* \tag{4.8}$$

corresponding to (3.22) and (3.23). The solution of these equations is straightforward, and we get

$$\begin{aligned} C_r &= 0 \text{ and } C_r = -\frac{C_R}{1+Q} \\ C_i &= -C_H \text{ and } C_i = -\frac{Q_*}{1+Q_*}\, C_H \end{aligned} \tag{4.9}$$

where Q_* is defined in (4.8). It is thus seen that the solution (4.9) is completely analogous to the previous, the only difference being the one between Q and Q_*. In order to evaluate the solutions

we need first of all to determine n, the order of the Bessel function, which in turn depends upon the lapse rate γ . The values n = 4 and 5 give the lapse rates $\gamma = 0.85 \times 10^{-2}$ and $\gamma = 0.68 \times 10^{-2}$, respectively. The corresponding values of q_r , evaluated from the tabulated values of the zeroes of the Bessel function, are given in Table 1.

n = 4	0.9495	1.3831	1.7966	2.2020	2.6034	3.0024	3.3999	3.7964	4.1921
n = 5	0.8771	1.2339	1.5700	1.8980	2.2218	2.5430	2.8677	3.1812	3.4989

Table 1.

Figure 3 shows the phase speed for the first three vertical modes for the case n = 5 ($\gamma = 0.68 \times 10^{-2}$ deg m^{-1}). A comparison with Figure 1 shows that the vertical variation of the static stability parameter has a very significant influence on the speed of propagation giving larger numerical values of C_r. The e - damping times for the same case are shown in Figure 4 which indicates that the e -damping times are larger for all wavelengths than those shown in Figure 2. The case n =4 ($\gamma = 0.85 \times 10^{-2}$ deg m^{-1}) is displayed in Figures 5 and 6 which shows that a reduction in the retrogression of the waves is found when γ is increased accompanied by a decrease in the e -damping time. A straightforward comparison with the case in which $\bar{\sigma}$ is kept constant is not possible because this case is not characterized by a constant lapse rate. In fact, the vertical distribution of the temperature in this case is such that a negative lapse rate exists in the lower layers of the atmosphere.

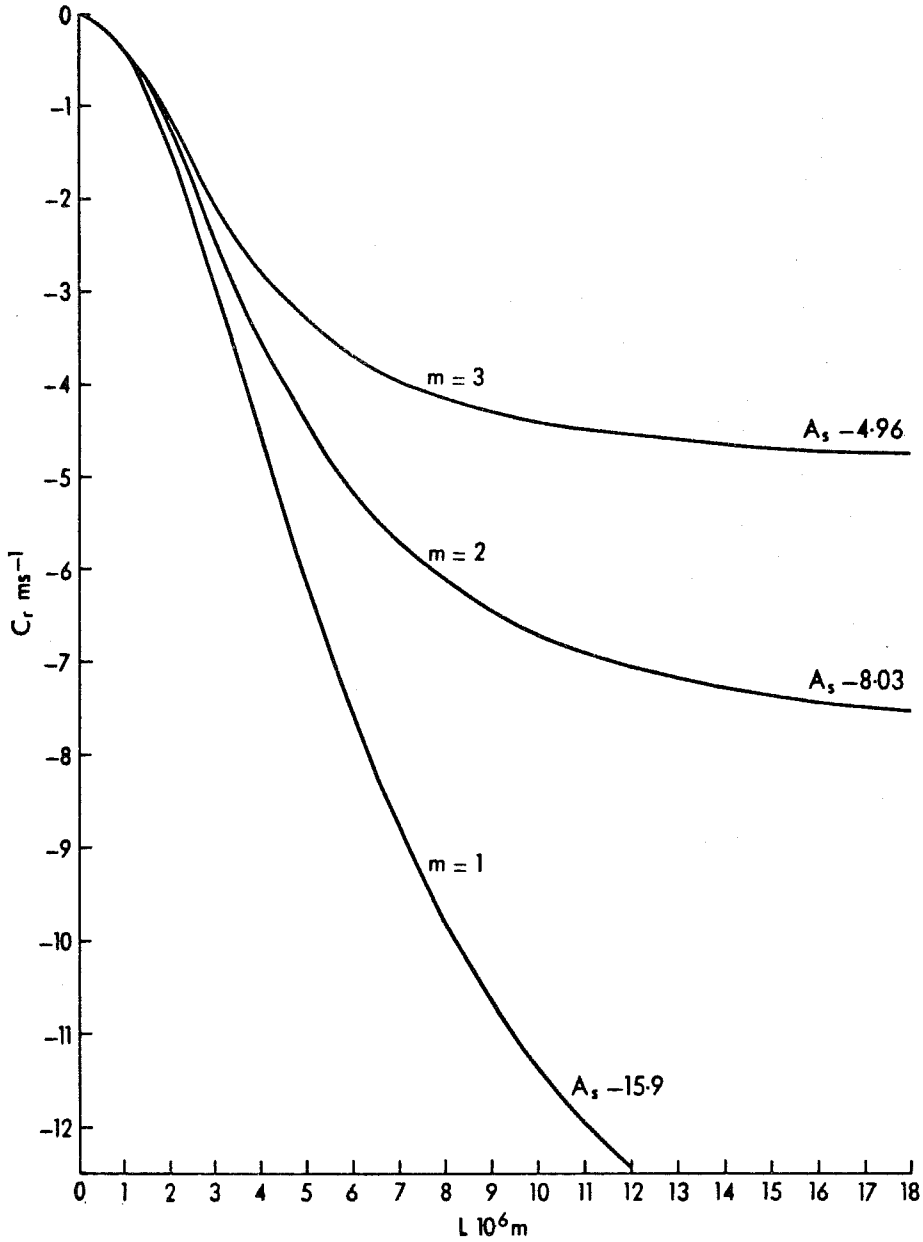

Fig.3: Real part of the phase speed in the case of a constant lapse rate (n = 5) as a function of wavelength for the first three vertical modes. Asymptotic values for large values of the wavelength are given on the curves.

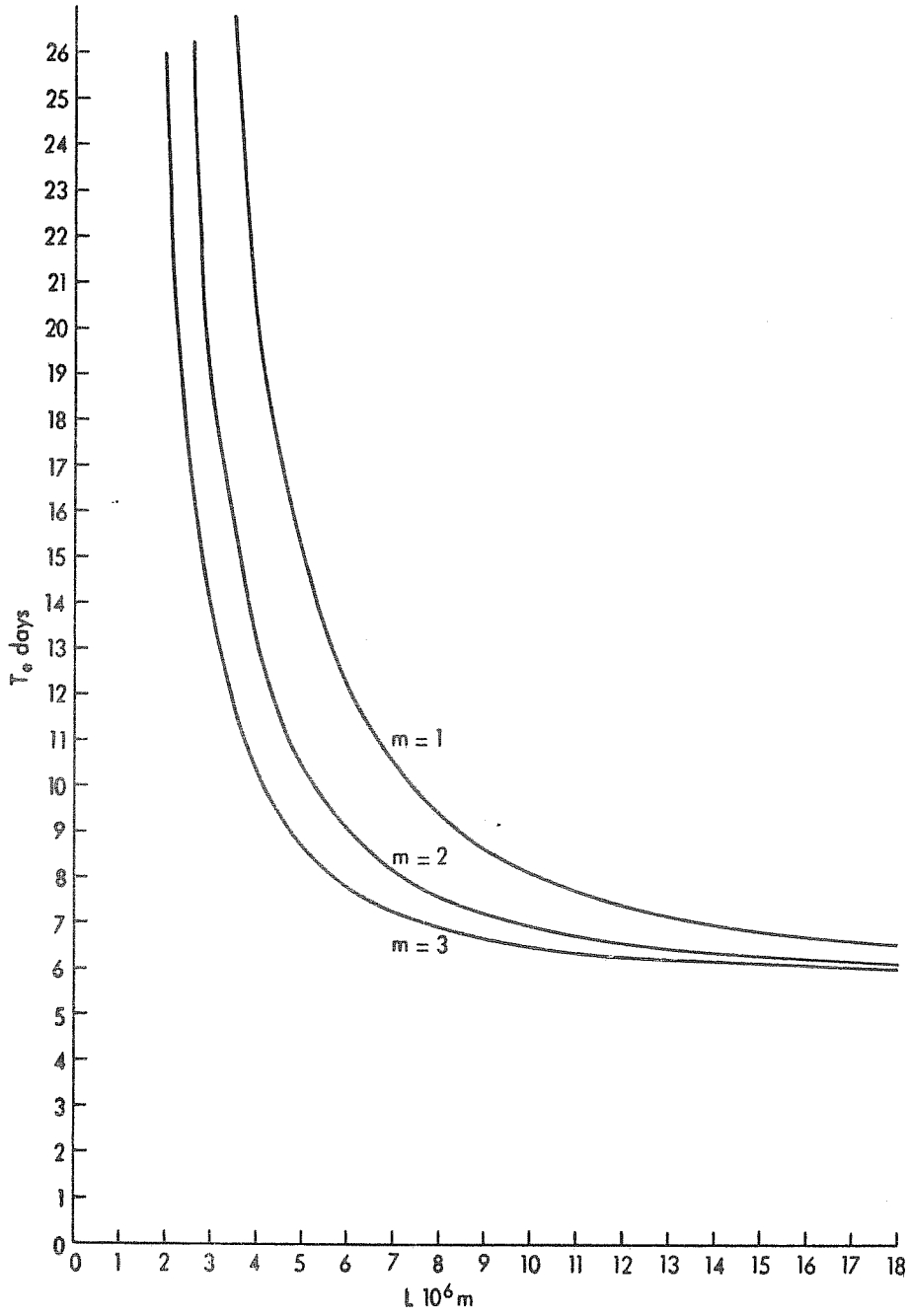

Fig.4: The e-folding time in days as a function of wavelength.
Same parameters as in fig.3.

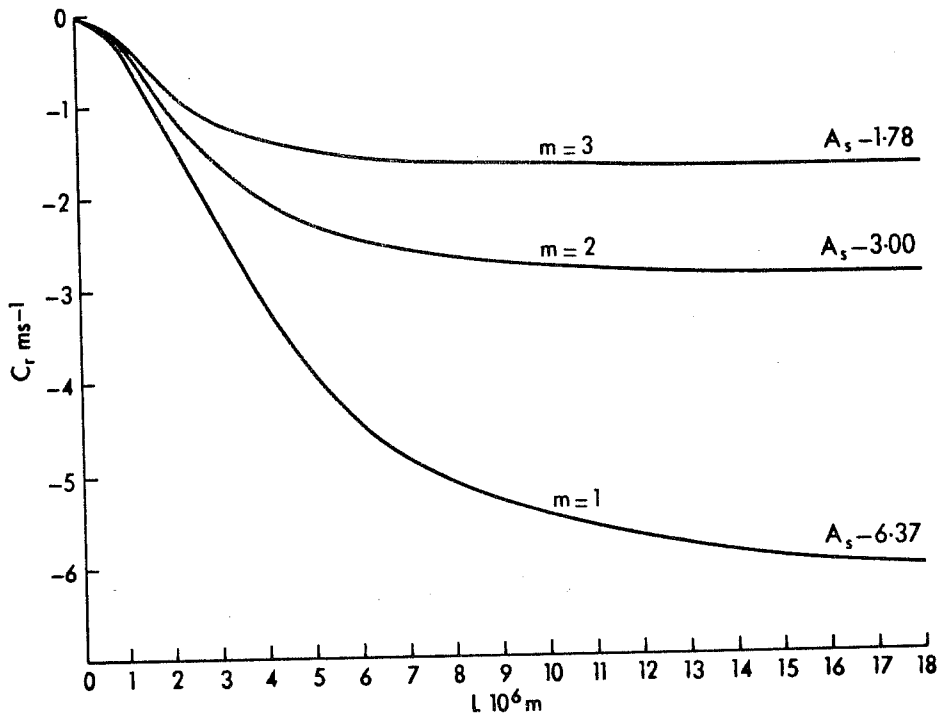

Fig.5: Real part of the phase speed in the case of a constant lapse rate (n = 4) as a function of wavelength for the first three vertical modes. Asymptotic values for large values of the wavelength are given on the curves.

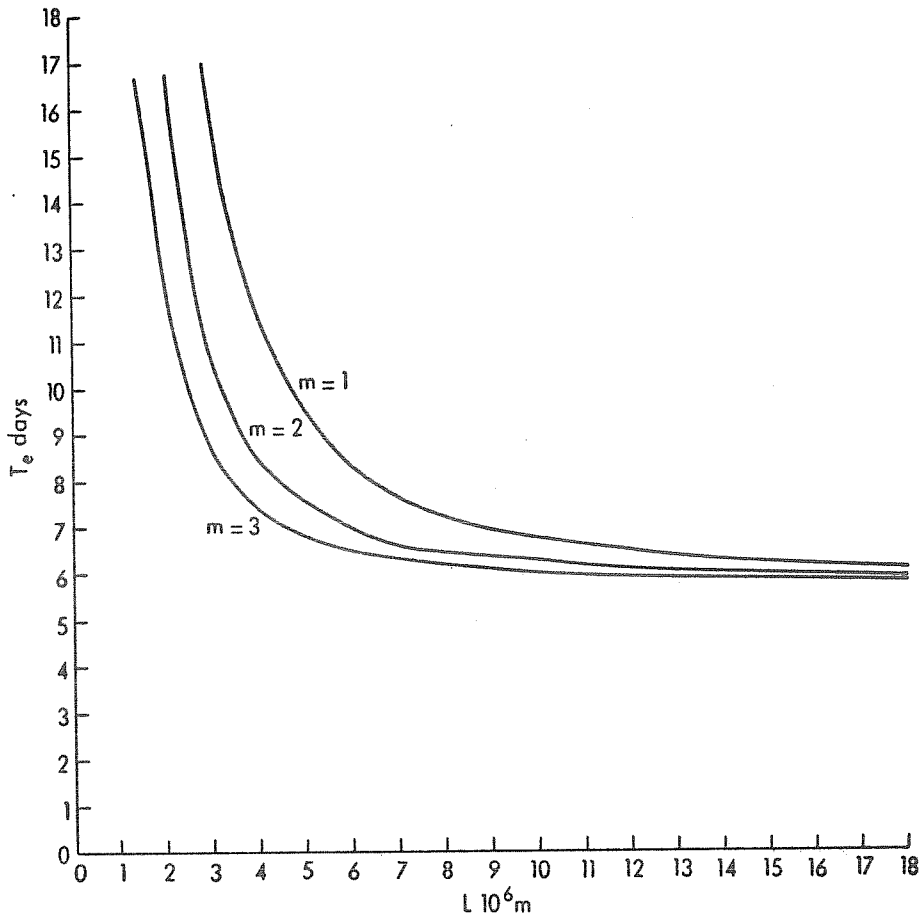

Fig.6: The e-damping time in days as a function of wavelength.
Same parameters as in fig.5.

5. Energetics of the Waves.

The inclusion of a heat source in the model indicates that there will be a non-zero generation of available potential energy. Similarily, the existence of a vertical velocity in the model guarantees that there will be an energy conversion between available potential energy and eddy kinetic energy. In view of the fact that the results in section 4 show that the constant lapse rate atmosphere is more realistic than the model with a constant static stability parameter we shall in this section calculate the generation of available potential energy, G(A), and the energy conversion C(A,K) using the results in section 4. For this purpose we need (4.5) for Ω . Introducting a new indpendent variable

$$y = 2nq\, p_*^{\frac{1}{2n}} \quad , \quad p_* = \left(\frac{y}{2nq}\right)^{2n} \tag{5.1}$$

we may write Ω in the form

$$\Omega = C \frac{1}{(2nq)^n}\, y^n J_n(y) \tag{5.2}$$

The amplitude of the geopotential, Φ_*, can be calculated from the vorticity equation (2.16) giving

$$\Phi_* = \frac{C_I^2}{p_o} \frac{1}{ik(C+C_R)} \frac{d\Omega}{dp_*} \tag{5.3}$$

or, upon evaluation,

$$\Phi_* = C \frac{C_I^2}{p_o} \frac{1}{ik(C+C_R)} \frac{(2nq)^n}{2n}\, y^{-(n-1)} J_{n-1}(y) \tag{5.4}$$

Assuming that

$$\omega = \Omega e^{ik(x-ct)} = \Omega \cos k(x-C_r t) e^{kC_i t} \tag{5.5}$$

we find

$$\Phi_* = -\frac{C_I^2}{p_o k} \frac{1}{(C_R+C_R)^2+C_i^2} (C_i \cos\varphi - (C_r + C_R)\sin\varphi) \frac{d\Omega}{dp_*} e^{kC_i t} \tag{5.6}$$

in which

$$\varphi = k(x-C_r t) \tag{5.7}$$

With these preparations it is straightforward to calculate

$$C(A,K) = -\frac{1}{gL}\int_0^1\int_0^L \Phi\,\frac{\partial\,\omega}{\partial p_*}\,dp_*dx \tag{5.8}$$

Inserting (5.5) and (5.6) into (5.8) we find

$$C(A,K) = +\frac{1}{2g}\,\frac{C_I^2}{p_o k}\,\frac{C_i}{(C_r+C_R)^2+C_i^2}\left(\int_0^1 (\frac{d\,\Omega}{dp_*})^2 dp_*\right)\,e^{2kC_i t} \tag{5.9}$$

or

$$C(A,K) = -\frac{C_I^2}{2gp_o k}\,\frac{1+Q_*}{Q_*}\,\frac{C_H}{C_R^2+C_H^2}\,e^{2kC_i t}\int_0^1 (\frac{d\Omega}{dp_*})^2\,dp_* \tag{5.10}$$

(5.10) shows that C(A,K) is negative for all scales. It is also apparent that C(A,K) will decrease exponentially with time because C_i is always negative. The conversion of energy from the eddy kinetic to the eddy available potential energy is induced by the Newtonian heating because C(A,K) is proportional to C_H. In order to make comparisons later with G(A) we shall evaluate the integral in (5.10). This can be done by straightforward methods using the transformation (5.1). We get:

$$I_1 = \int_0^1 (\frac{d\Omega}{dp_*})^2\,dp_* = \int_0^{2nq} \frac{(2nq)^{4n}}{4n^2}\,y^{2-4n}\,(\frac{d\Omega}{dy})^2\,\frac{2n}{(2nq)^{2n}}\,y^{2n-1}\,dy \tag{5.11}$$

which upon evaluation can be written in the form

$$I_1 = \frac{C^2}{2n}\int_0^{2nq} y\left[J_{n-1}(y)\right]^2 dy \tag{5.12}$$

or

$$I_1 = nq^2C^2\left[J_{n-1}(2nq)\right]^2 \tag{5.13}$$

where we have made use of the fact that $J_n(2nq) = 0$.

The final result is therefore

$$C(A,K) = - \frac{C_I^2}{2gp_o k} \quad \frac{1+Q_*}{Q_*} \quad \frac{C_H}{C_R^2+C_H^2} e^{2kC_i t} \; ng^2 \wp^2 \left[J_{n-1}(2nq)\right]^2 \tag{5.14}$$

The next problem is to evaluate the generation of eddy available potential energy. Directly from the definition of G(A) we find

$$G(A,K) = - \frac{1}{gL} \int_o^L \int_o^{p_o} \frac{\gamma}{\bar{\sigma}} \left(\frac{\partial \Phi}{\partial p}\right)^2 dpdx \tag{5.15}$$

which shows immediately that $G(A) < 0$ due to the Newtonian form of the heating.

The integral (5.15) can be evaluated using the same transformations as before. In this connection it must be recalled that $\bar{\sigma}$ is a function of pressure. We note that

$$\bar{\sigma} = \sigma_o p_*^{\frac{1}{n} - 2} \tag{5.16}$$

giving

$$\frac{1}{\bar{\sigma}} = \frac{1}{\sigma_o} p_*^{2-\frac{1}{n}} = \frac{1}{\sigma_o} \left(\frac{y}{2nq}\right)^{4n-2} \tag{5.17}$$

In (5.15) we introduce first of all p_* as the independent variable giving

$$G(A) = - \frac{\gamma}{gLp_o} \int_o^L \int_o^1 \frac{1}{\bar{\sigma}} \left(\frac{\partial \Phi}{\partial p_*}\right)^2 dp_* dx \tag{5.18}$$

Replacing p_* by y as the independent variable we get using (5.1)

$$G(A) = - \frac{\gamma}{gp_o L} \int_o^L \int_o^{2nq} \frac{1}{\bar{\sigma}} \frac{(2nq)^{2n}}{2n} y^{1-2n} \left(\frac{\partial \Phi}{\partial y}\right)^2 dydx \tag{5.19}$$

In order to evaluate (5.19) it is most convenient to make use of (5.6) which, using (5.1) again, can be written in the form

$$\Phi_* = - \frac{C_I^2}{p_o k} \frac{1}{(C_R+C_R)^2+C_i^2} (C_i \cos\varphi - (C_r+C_R) \sin\varphi) \frac{(2nq)^{2n}}{2n} y^{1-2n} \frac{d\Omega}{dy} \tag{5.20}$$

(5.20) is differentiated with respect to y and substituted in (5.19) together with the expression (5.17) for $1/\bar{\sigma}$. The result is

$$G(A) = -\frac{C_I^4}{2gp_o kC_g^2}\left(\frac{1+Q_*}{Q_*}\right)^2 \frac{C_H}{C_R^2+C_H^2}\frac{(2nq)^{2n+2}}{8n^3}\int_o^{2nq} y^{2n-1}\left[\frac{d}{dy}\left(y^{1-2n}\frac{d\Omega}{dy}\right)\right]^2 dy \qquad (5.21)$$

The remaining problem is to evaluate the integral

$$I_2 = \int_o^{2nq} y^{2n-1}\left[\frac{d}{dy}\left(y^{1-2n}\frac{d\Omega}{dy}\right)\right]^2 dy \qquad (5.22)$$

(5.22) is evaluated using the expression (5.2) for $\Omega = \Omega(y)$, and it turns out that

$$I_2 = \frac{\mathcal{E}^2}{(2nq)^{2n}}\int_o^{2nq} y\left[J_n(y)\right]^2 dy \qquad (5.23)$$

which can be evaluated directly giving

$$I_2 = \frac{\mathcal{E}^2}{(2nq)^{2n}}\, 2n^2q^2(-J_{n-1}(2nq)J_{n+1}(2nq)) \qquad (5.24)$$

where we once again have made use of the fact that $J_n(2nq) = 0$. It can furthermore be shown quite easily that

$$J_{n-1}(2nq)+J_{n+1}(2nq) = 0 \qquad (5.25)$$

(5.25) follows immediately from the general formula

$$y(J_{n-1}(y)+J_{n+1}(y)) = 2nJ_n(y) \qquad (5.26)$$

where the right hand side is zero for $y = 2nq$. Combining (5.25) with (5.24) the following expression for G(A) is found:

$$G(A) = -\frac{C_I^4}{2gp_o kC_g^2}\left(\frac{1+Q_*}{Q_*}\right)^2 \frac{C_H}{C_R^2+C_H^2}\, nq^4C^2\left[J_{n-1}(2nq)\right]^2 \qquad (5.27)$$

The expressions (5.14) and (5.27) can be used to explore the energetics of the waves. We note first of all that

$$\frac{G(A)}{C(A,K)} = 1+Q_* = 1+ \frac{q_r^2}{C_g^2} \frac{f_0^2}{k^2} \tag{5.28}$$

which shows that $G(A) = C(A,K)$ for $L = 0$. Figure 7 shows the relation (5.28) for the first three modes indicating that $|G(A)| > |C(A,K)|$ for all values of the wavelength. Both Figure 7 and (5.28) show that the ratio of the generation and the conversion is larger for the higher vertical modes than for the smaller modes for a given value of the wavelength. The reason is that q_r increases with the vertical mode number. The interpretation of this result is that the energy reservoir of eddy available potential energy is being depleted due to the Newtonian heating. As the evaluation shows this is not only due to the fact that $G(A) < 0$ which represents a loss of eddy available potential energy. This loss is partially compensated by the conversion of eddy kinetic to eddy available potential energy. However, the compensation is not enough to prevent a decrease of the eddy available potential energy which therefore in the actual atmosphere must be replenished by some other process. This process is naturally the conversion of zonal to eddy available potential energy. Figure 7 shows furthermore that the higher modes lose more eddy available potential energy than the lower vertical modes for the same value of the wavelength.

A further illustration of the behaviour of G(A) and C(A,K) can be given by noting that $G(A) = C(A,K)$ for $L = 0$. We may thus normalize the expressions by determining the arbitrary constant C in such a way that $G(A) = C(A,K) = 1$ for $L = 0$. This procedure leads to

$$C^2 = \frac{2gp_0\gamma}{nC_g^2\left[J_{n-1}(2nq)\right]^2} \tag{5.29}$$

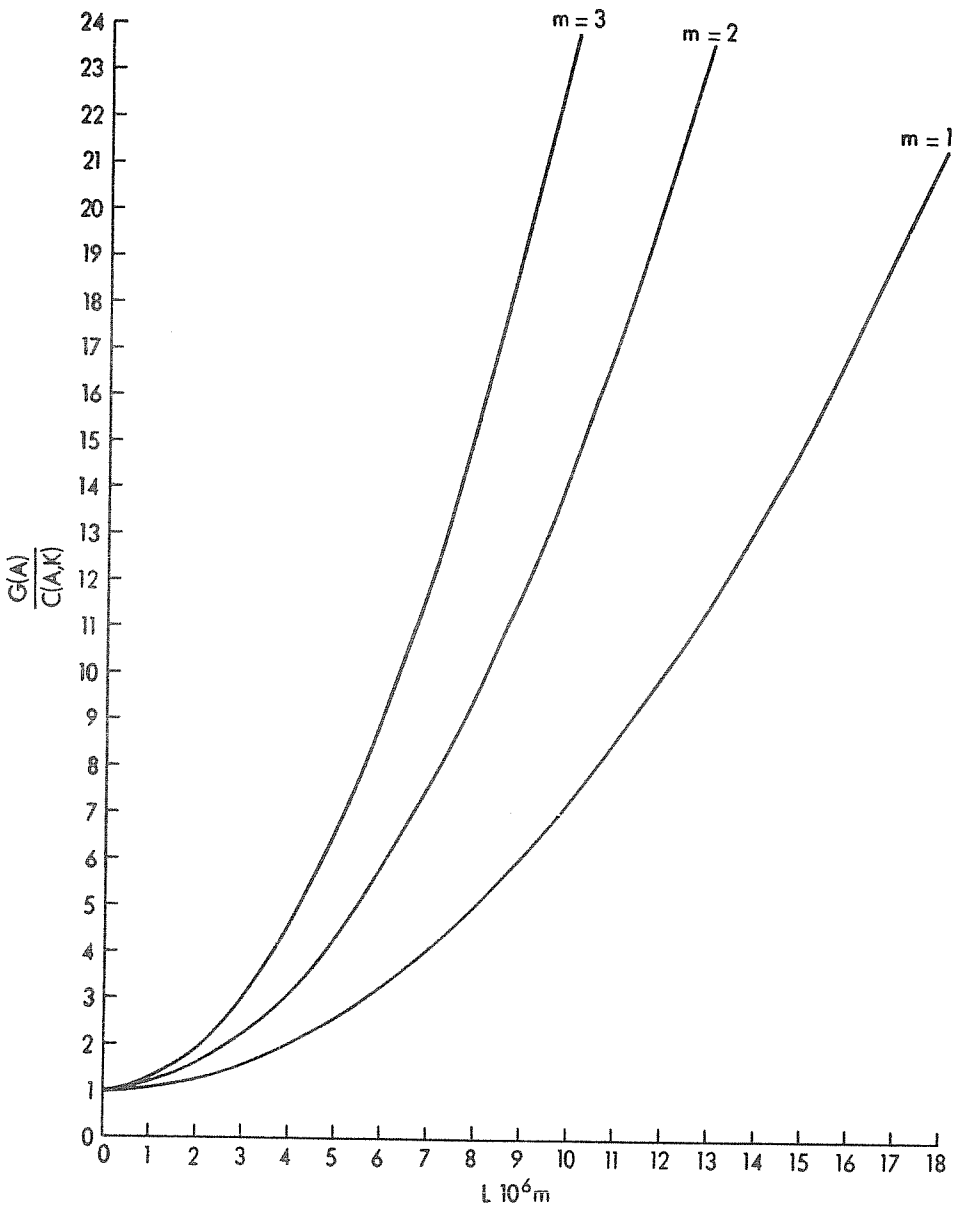

Fig.7: The ratio between the generation of available potential energy and the conversion between available potential and kinetic energy as a function of wavelength for the first three vertical modes.

With this value of C^2 we may calculate -G(A) and -C(A,K) as a function of wavelength for the various vertical modes. These curves are shown in Figures 8, 9 and 10 for the first, second and third vertical modes, respectively. The curves show that -C(A,K) decreases monotonically with increasing wavelength to an asymptotic value which depends on the vertical mode. The asymptotic value is derived from (5.14) by letting k= 0. Using (5.29) for C^2 we find that

$$-C(A,K)\Big|_{k=0} = \frac{f_o^2\gamma^2}{\beta^2}\frac{q^2}{C_g^2} \tag{5.30}$$

showing that the higher vertical modes (q large) have larger asymptotic values as is also seen from Figures 8, 9 and 10. The same figures show also that - G(A) has a minimum for each vertical mode. The position of the minimum moves toward smaller values of the wavelength as the higher vertical modes are considered. This behaviour for the vertical modes can be derived from (5.27) by finding the value of k for each G(A) becomes a minimum. Using (5.29) for C^2 we find that - G(A) can be written in the form

$$-G(A) = \frac{f_o^4\gamma^2q^4}{C_g^4}\,F(k) \tag{5.31}$$

where

$$F(k)= \frac{(1+\frac{C_g^2}{q^2f_o^2}\,k^2)^2}{(\beta^2+\gamma^2k^2)k^2} \tag{5.32}$$

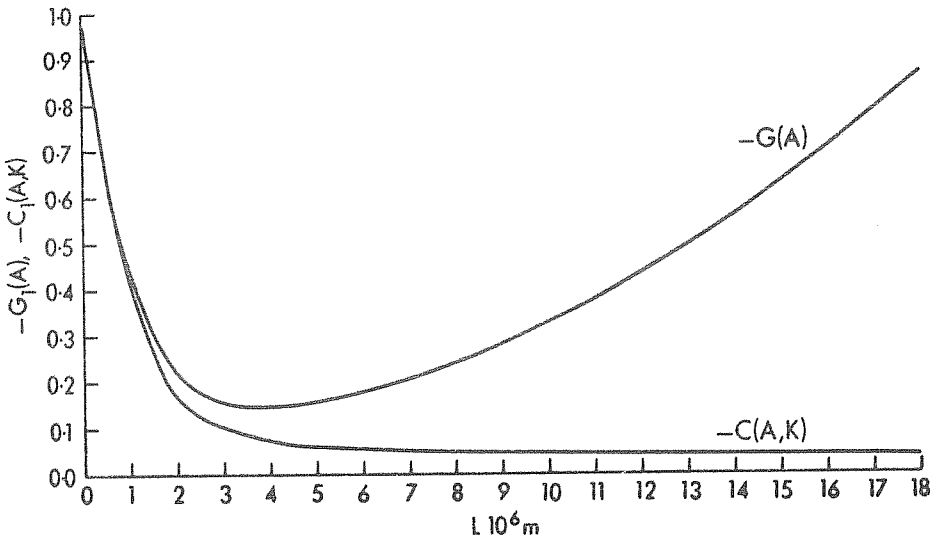

Fig.8: The destruction of available potential energy and the conversion from kinetic to available potential energy as a function of wavelength for the first vertical mode.
Values are normalized to unity at L = 0.

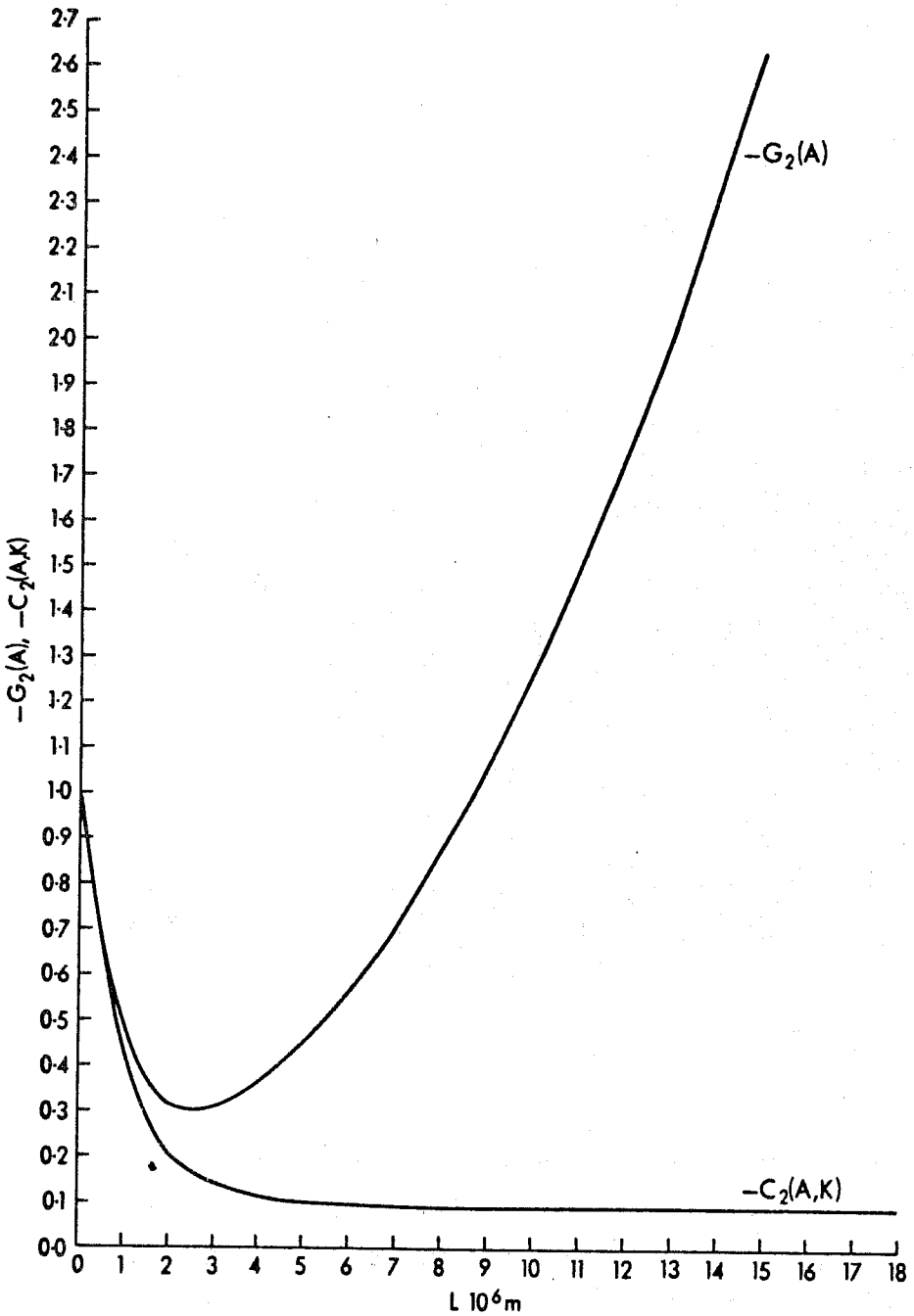

Fig.9: As fig.8 but for the second vertical mode.

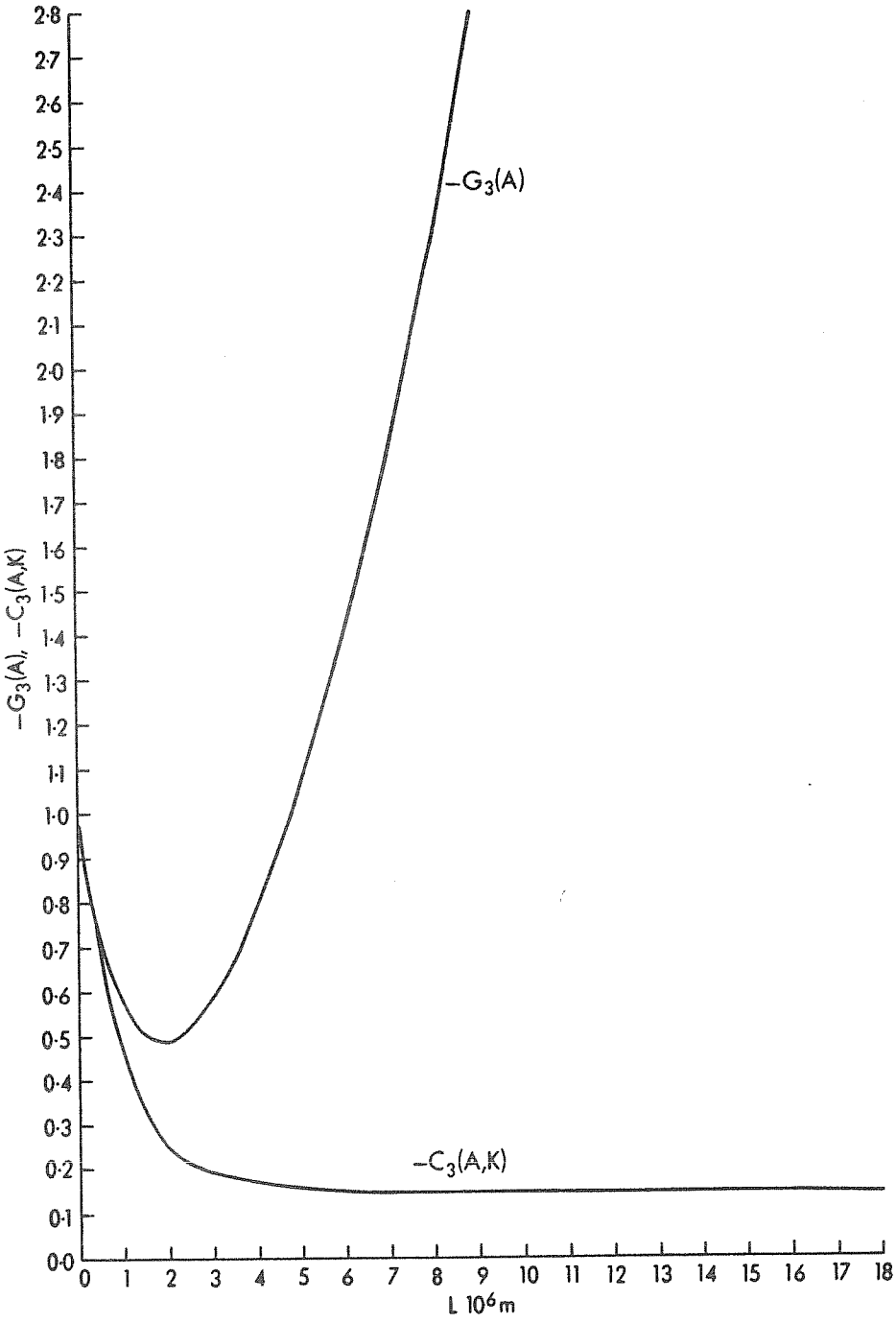

Fig.10: As fig.8 but for the third vertical mode.

Differentiation of (5.32) with respect to k shows that the derivative is zero when

$$k^2 = \frac{1}{\frac{C_g^2}{q^2 f_o^2} - 2\frac{\gamma}{\beta^2}} \tag{5.33}$$

or that the wavelength for which -G(A) is a minimum is

$$L_{min} = 2\pi\left(\frac{C_g^2}{q^2 f_o^2} - 2\frac{\gamma^2}{\beta^2}\right)^{\frac{1}{2}} \tag{5.34}$$

Since q increases when we consider higher and higher vertical modes, it is seen from (5.34) that L_{min} will decrease as shown on Figures 8, 9 and 10. The same formula shows also that there is an upper limit for q if - G(A) should have a minimum, because it must be required that the radicand in the square root in (5.34) must be positive. The maximum value of q is

$$q_{max} = \left(\tfrac{1}{2}\frac{\beta^2}{\gamma 2}\frac{C_g^2}{f_o^2}\right)^{\frac{1}{2}} \tag{5.35}$$

Using the same numerical values as before we find that $q_{max} = 3.4$. Comparing with the values of q shown in Table 1 (n = 4) we find that the first seven vertical modes will have a minimum value of -G(A). In the general case we find after some calculations that

$$-G(A)_{min} = \frac{4 f_o^2 \gamma^2}{C_g 4\beta^2} q^2\left(\frac{C_g^2}{f_o^2} - \frac{\gamma^2}{\beta} 2q^2\right) \tag{5.36}$$

It is seen that $-G(A)_{min} = 1$ when $q = q_{max}$.

The main results of the investigation of the energetics of the waves are thus that G(A) and C(A,K) are negative, that A will experience a loss of energy because G(A) is numerically larger than C(A,K), and that -G(A) for the first vertical modes has a minimum which varies between about 4000km for the first mode and 2000km for the third mode.

6. Newtonian Heating with Non-Zero Basic Flow.

The solutions described in sections 4 and 5 are obtained in the case where the basic state is a state of rest. The influence of Newtonian heating on the development of baroclinic waves has been investigated by Wiin-Nielsen et al (1967) for the two level quasi-geostrophic model. The general result obtained in that case is that the Newtonian heating makes all waves longer than a critical wave-length unstable. We shall here reconsider the problem and investigate the degree of instability as well as the influence of the Newtonian heating on the speed of propagation of the waves.

The same question has been investigated by Döös (1969) who solved the perturbation equations in a model with continuous vertical stratification and forced by a heating depending on the surface temperature and having a specified vertical distribution. In the detailed calculations the heating was proportional to pressure. The present study in which Newtonian heating is used should supplement his result.

For our purpose we shall solve the perturbation equations directly and obtain a formula for the complex wave speed. The perturbation equations are (see (2.8) and (2.9) in Wiin-Nielsen et al. 1967).

$$\frac{\partial \Phi}{\partial t}_{*} + (U_{*}-C_R)\frac{\partial \Phi_{*}}{\partial x} + U_T \frac{\partial \Phi T}{\partial x} = 0 \tag{6.1}$$

$$\frac{\partial \Phi T}{\partial t} + \left(U_{*} - \frac{k^2}{k^2+q^2} C_R\right)\frac{\partial \Phi T}{\partial x} \quad \frac{k^2-q^2}{k^2+q^2} U_T \frac{\partial \Phi_{*}}{\partial x} = -\frac{q^2}{k^2+q^2}\gamma\Phi\, T \tag{6.2}$$

in which the subscripts$_{*}$ and T are defined as follows

$$( )_* = \tfrac{1}{2}\left[( )_1 + ( )_3\right]$$
$$( )_T = \tfrac{1}{2}\left[( )_1 - ( )_3\right] \qquad (6.3)$$

and where the perturbations have the form

$$\Phi_{*,T} = \Phi_{*,T}\, e^{ik(x-ct)} \qquad (6.4)$$

while

$$q^2 = \frac{2f_o^2}{\sigma p^2} \qquad (6.4)$$

Introducing (6.4) in (6.1) and (6.2) and proceeding in the usual way we can calculate the complex wave speed from the frequency which with the notation $x = C - U_*$ is

$$X^2 + \left\{\frac{2k^2+q^2}{k^2+q^2}C_R + i\,\frac{q^2}{q^2+k^2}C_H\right\} X + \frac{k^2}{k^2+q^2}C_R^2 - \frac{k^2-q^2}{k^2+q^2}\,U_T^2 + i\frac{q^2}{k^2+q^2}\,U_T^2 = 0 \qquad (6.5)$$

The solution to (6.5) is most conveniently written in the form

$$X = \begin{cases} \tfrac{1}{2}\left\{-\dfrac{1+2n^2}{1+n^2}\,C_R + \dfrac{a}{1+n^2} + i\,\dfrac{b-C_H}{1+n^2}\right\} \\ \tfrac{1}{2}\left\{-\dfrac{1+2n^2}{1+n^2}C_R - \dfrac{a}{1+n^2} - i\,\dfrac{b+C_H}{1+n^2}\right\} \end{cases} \qquad (6.6)$$

in which

$$n = \frac{k}{q}\ ,\quad a = \left(\frac{S+Q}{2}\right)^{\frac{1}{2}}\ ,\quad b = \left(\frac{S-Q}{2}\right)^{\frac{1}{2}} \qquad (6.7)$$

and

$$Q = C_R^2 - C_H^2 - 4(1-h^2)\,U_T^2 \qquad (6.8)$$

and

$$S = (Q^2 + 4C_R^2 C_H^2)^{\frac{1}{2}} \qquad (6.9)$$

It is seen that the second solution in (6.6) represents damped waves in all cases because the imaginary part is negative. The expression for the second solution shows also that the damped wave will move slower from west to east because of the term $-a/(1+n^2)$.

The first solution in (6.6) will represent an instability if $b > C_H$. It is easily shown that the inequality is satisfied if and only if

$$k < q \tag{6.10}$$

It is thus seen that instability occurs for all wavelengths larger than

$$L_{Cr} = \frac{2\pi}{q} \tag{6.11}$$

On the other hand, if the Newtonian heating is excluded ($C_H = 0$) we find that $S = Q$, $b = 0$ and $a = Q_*^{\frac{1}{2}}$ where

$$Q_* = C_R - 4(1-n^2)U_T^2 \tag{6.12}$$

In this case we get the well known solution

$$X_* = \begin{cases} \frac{1}{2}\left\{ -\frac{1+2n^2}{1+n^2} C_R + \frac{Q_*^{\frac{1}{2}}}{1+n^2} \right\} \\ \frac{1}{2}\left\{ -\frac{1+2n^2}{1+n^2} C_R - \frac{Q_*^{\frac{1}{2}}}{1+n^2} \right\} \end{cases} \tag{6.13}$$

In order to compare the degree of instability we have computed the e-folding time $T_e = \frac{1}{kC_i}$ from (6.6) and (6.13) in the regions of

instability. For this purpose the following values were adopted: $\beta = 16 \times 10^{-12} m^{-1} sec^{-1}$, $\gamma = 2 \times 10^{-6} sec^{-1}$, $q = 2 \times 10^{-6} m^{-1}$ and $U_T = 15 msec^{-1}$, corresponding approximately to a vertical wind shear of 4 $msec^{-1} km^{-1}$. The result is given in Table 2, in which T_e is expressed in days.

It is seen that the heating in the common region of instability in general decreases the degree of instability. This is true for all the values listed in the table, $4 \times 10^6 \leq L \leq 8 \times 10^6$, but there are small regions in which the opposite must be true for the simple reason that T_e in the case of no heating has two vertical asymptotes at the values of L which represent the transition from instability to stability. These values of L are determined by the relation $Q_* = 0$ and for the same values of the parameters one finds the values L = 3192 km and L = 8330 km. On the other hand, the curve for T_e in the case of heating has a vertical asymptote at L = 3142 km. However, in the small regions in which T_e (heating) $< T_e$ (no heating) the values of T_e will be so large that the physical significance is doubtful. Table 2 shows also that the instability created by the heating at large wavelengths is very weak with e -folding times of a week or more.

While the influence of the Newtonian heating thus is of a minor nature with respect to the instability it is much more interesting to investigate the phase speed. The formulas are (6.6) and (6.13) which show that the important contribution from the heating comes from the term $a/(1 + n^2)$. The main point in (6.6) is that we may be permitted to disregard the solution which corresponds to the damped wave. The reason for this is that the time required to decrease the amplitude by a factor of e is relatively short as

Wavelength, 10^6m	4	5	6	7	8	9	10	12	14	16	18	20
T_e, days (heating)	0.75	0.66	0.73	0.95	1.90	7.06	15.47	40.07	79.15	138	233	339
T_e, days (no heating)	0.69	0.61	0.67	0.85	1.70	-	-	-	-	-	-	-

Table 2.

Wavelength, 10^6m	1	2	3	4	5	6	7	8	9	10	12	14	16	18	20
T_e (days)	64.0	20.4	9.2	0.65	0.57	0.61	0.75	1.21	2.24	2.65	2.88	2.95	2.96	2.96	2.96

Table 3.

seen from Table 3. This is particularly so for the medium and very long waves which are of special interest here. The phase speed of the damping waves is very large and negative for long waves as seen from (6.6) but this fact is supposedly of little importance since these waves are damped relatively quickly.

The amplifying waves on the other hand will move relatively slowly from east to west for large values of the wavelength due to the compensating effect between the first two terms in (6.6). This is clearly seen from Table 4 in which we have listed the values of these terms as a function of wavelength. The first term is the familiar beta-effect, while the second is the effect of the heating.

Some years ago the author (Wiin-Nielsen, 1970 and 1971) investigated the motion of very long transient waves by the use of the perturbation method and employing a basic state of rest and a vertical stratification characterized by a constant lapse rate. It was found in these studies that the only vertical mode which moved with a large phase speed from east to west was the basic vertical mode corresponding to the mode found in a homogeneous fluid with a free surface. This mode is very similar to the nondivergent Rossby mode modified by the influence of surface pressure changes.

In the present study we find that the second solution in (6.13) in the case of no heating will approach the Rossby wave speed - C_R when $k \neq 0$ as is well known. This solution corresponds in the case of Newtonian heating to the damped solution, and it will therefore not exist in the model atmsophere after a certain period of time.

Wavelength, 10^6m	1	2	3	4	5	6	7	8
$-(2n^2+1)C_R/2(n^2+1)$	-0.38	-1.37	-2.74	-4.43	-6.43	-8.76	-11.46	-14.54
$a/2(n^2+1)$	4.09	5.26	2.50	0.14	0.27	0.50	0.98	2.44
Sum	3.71	3.89	-0.24	-4.29	-6.16	-8.26	-10.48	-12.10

Wavelength, 10^6m	9	10	12	14	16	18	20
$-(2n^2+1)C_R/2(n^2+1)$	-17.98	-21.82	-30.67	-41.10	-53.12	-66.74	-81.95
$a/2(n^2+1)$	7.48	12.86	23.31	34.62	47.20	61.20	76.70
Sum	-10.50	-8.96	-7.36	-6.48	-5.92	-5.54	-5.25

Table 4.

On the other hand, the first solution in (6.13) will for large values of the wavelength ($k \to 0$) approach the value $-\beta/2q^2$ because $Q_*^{\frac{1}{2}}$ in (6.12) will approach $(C_R^2 - 4\,U_T^2)^{\frac{1}{2}} \approx C_R$. This solution will correspond to the first solution in (6.6). Since the wave is amplifying for all values $k < q$, i.e. the long waves, it will exist in the atmosphere, and its phase speed will be given by the values listed in Table 4.

The above result appears to be of importance because it indicates that the main result of the Newtonian heating is to give all the waves larger than a critical wavelength a complex phase speed. The solution which in the adiabatic case behaves similarly to the nondivergent Rossby waves, i.e. $X_r \to -\infty$, $k \to 0$, becomes a damped wave with e -damping time of less than three days, and it will thus not appear in the model with any significant amplitude. On the other hand, the unstable solution will move slowly in the negative direction relative to the basic current at the mid-level. The results of this analysis indicate therefore that a model with Newtonian heating should not suffer from an excessive retrogression of the ultra-long waves, which has been a constant problem with adiabatic models. It must on the other hand be stressed that these results are based on the theory of small perturbations and on a particular form of heating. The Newtonian form adopted here is certainly a simplification, but there are good reasons to believe that it is of the correct form for the large-scale motion because on this scale the heating is dominated by the interaction with the surface of the earth.

7. Some Tendency calculations.

The earlier sections of this paper have been devoted to an analysis of the direct influence of Newtonian heating on atmospheric waves. In addition, it is of interest to investigate the vertical velocities, the tendencies in geopotential and/or pressure and the temperature tendencies which are caused directly by the heating. Calculations of this kind have been carried out by Döös (1961) who found that such changes are very scale dependent. Our results will confirm his conclusions but will give some additional results.

In order to isolate the effects of heating we shall disregard advection and thus use the following simplified quasi-geostrophic equations

$$\begin{aligned} \frac{\partial \nabla^2 \Phi}{\partial t} &= f_o^2 \frac{\partial \omega}{\partial p} \\ \frac{\partial}{\partial t}\left(\frac{\partial \Phi}{\partial p}\right) + \bar{\sigma}\,\omega &= -\frac{R}{C_p}\,\frac{1}{p}\,H \end{aligned} \tag{7.1}$$

in which we have neglected the beta-effect. From the system (7.1) we eliminate Φ and obtain the following equation for ω :

$$f_o^2 \frac{\partial^2 \omega}{\partial p^2} + \bar{\sigma}\,\nabla^2 \omega = -\frac{R}{C_p}\,\frac{1}{p}\,\nabla^2 H \tag{7.2}$$

The procedure will be to specify the diabatic heating H, solve (7.2) for ω with the boundary conditions that ω vanishes at the top of the atmosphere and at the standard pressure $p = p_o$ at the ground, and to calculate the tendencies for Φ from anyone of the two equations in (7.1). In order to keep the calculations relatively simple we shall specify the heating in the form

$$H = H_o \left(\frac{p}{p_o}\right)^{\alpha} \sin kx \sin my \tag{7.3}$$

in which H_o is the maximum heating at p= po, while α is a constant. The two constants k and m are the wave numbers in the x and y directions, respectively. We note that a large value of α means a rapid decrease of H with height. Solutions to (7.2) of the form

$$\omega = \Omega(p) \sin kx \sin my \tag{7.4}$$

will exist. Inserting (7.3) and (7.4) in (7.2) we get:

$$\frac{f_o^2}{p_o^2} \frac{d^2\Omega}{dp^{*2}} - \bar{\sigma}s^2\Omega = \frac{R}{C_p} \frac{s^2}{p_o} H_o p_*^{\alpha-1} \tag{7.5}$$

in which $s^2 = k^2 + m^2$.

The solution of (7.5) depends on how $\bar{\sigma} = \bar{\sigma}(p)$ varies with pressure. A relatively realistic specification is

$$\bar{\sigma} = \sigma_o p_*^{-2} \tag{7.6}$$

in which case (7.5) takes the form

$$\frac{f_o^2}{p_o^2} \frac{d^2\Omega}{dp_*^2} - \frac{\sigma_o s2}{p_*^2} \Omega = \frac{R}{C_p} \frac{s^2}{p_o} H_o p_*^{\alpha-1} \tag{7.7}$$

The solution to (7.7) is easy to obtain, and after the integration constants have been determined in such a way that the boundary conditions are satisfied we find that

$$\Omega = A(p_*^{\alpha+1} - p_*^{\delta}) \tag{7.8}$$

in which

$$\delta = \tfrac{1}{2} + (\tfrac{1}{4} + \frac{\sigma_o p_o^2}{f_o^2} s^2)^{\frac{1}{2}} \tag{7.9}$$

and

$$A = \frac{R}{C_p} \frac{s^2}{p_o} \frac{H_o}{\frac{f_o^2}{p_o^2}\alpha(\alpha+1) - \sigma_o s^2} \tag{7.10}$$

Using (7.9) we may also write (7.10) in the form

$$A = \frac{R}{C_p} \frac{s^2}{f_o^2} \frac{H_o\, p_o}{\alpha(\alpha+1) - (\delta-1)\delta} \tag{7.11}$$

It is seen from (7.11) that A goes to infinity if $\alpha = \delta-1$. However, in this case the parenthesis in the expression for Ω is identically zero, and Ω becomes simply undefined. For a given value of α we can calculate the corresponding value of s for which Ω is undefined by setting $\delta = \alpha+1$ in (7.9). We find

$$s^2 = \frac{f_o^2}{\sigma_o p_o^2}\alpha(\alpha+1) \tag{7.12}$$

Introducing a horizontal effective wavelength by the relation

$$L = \frac{2\pi}{s} \tag{7.13}$$

we find

$$L = 2\pi\left(\frac{\sigma_o p_o^2}{f_o^2}\frac{1}{\alpha(\alpha+1)}\right)^{\frac{1}{2}} \tag{7.14}$$

If $\delta < \alpha+1$ it is seen that $A > 0$ and (6.8) shows that $\Omega < 0$ for all p_*. On the other hand, if $\delta > \alpha+1$ we find $A < 0$, but according to (6.8) we will still find $\Omega < 0$ for all p_*, because $p_*^{\alpha+1} > p_*^{\delta}$ for $0 < p_* < 1$ in this case. Figure 11 shows the vertical distribution of $-\Omega$ for two cases in which L = 1000km and L = 10000 km, while $\alpha = 3$ $\sigma_o = 2$ MTS units and $H_o = 10^{-1}$kj t^{-1}sec^{-1}

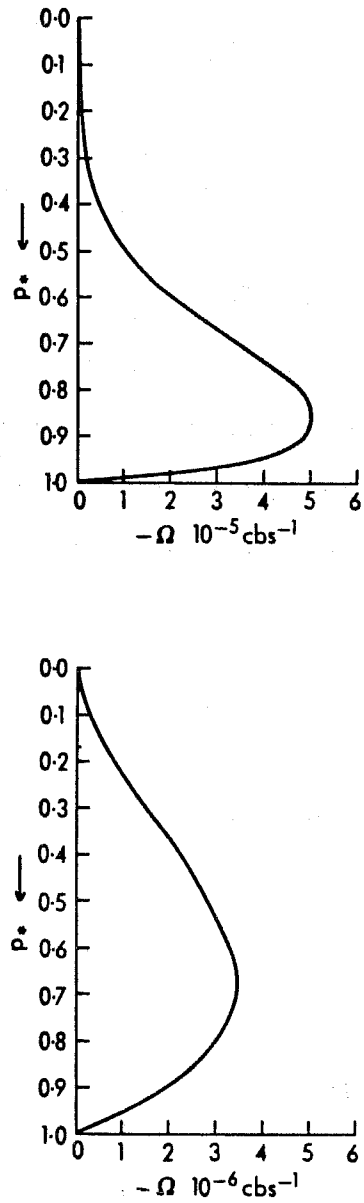

Fig.11: The negative values of the vertical p-velocity as a function of normalized pressure. Parameters: $\alpha = 3$, $\sigma_o = 2$, $H_o = 10^{-1}$, $L = 10^6$ (upper part), $L = 10^7$ (lower part). All values in MTS-units.

in both cases. It is seen that the largest values of $-\Omega$ are obtained for the smaller horizontal scale. The position of the maximum for $-\Omega$ is obtained from (7.8), and it is found that

$$p_{*,max} = \left(\frac{\delta}{\alpha+1}\right)^{\frac{1}{\alpha-\delta+1}} \tag{7.15}$$

while the maximum value of Ω is

$$\Omega_{max} = A\left[\left(\frac{\delta}{\alpha+1}\right)^{\frac{\alpha+1}{\alpha-\delta+1}} - \left(\frac{\delta}{\alpha+1}\right)^{\frac{\delta}{\alpha-\delta+1}}\right] \tag{7.16}$$

Figure 12 shows in the upper part the maximum value of $-\Omega$ as a function of wavelength for $\sigma_o = 2$, $\alpha = 3$, and $H_o = 10^{-1}$ indicating that $-\Omega_{max}$ decreases with increasing wavelength. The lower part of Figure 12 shows the position of the maximum as a function of wavelength. It is seen that the maximum occurs for smaller values of p_* as the wavelength increases.

The geopotential tendency is obtained from the vorticity equation in (7.1). Writing the tendency in the form

$$\frac{\partial \Phi}{\partial t} = \frac{\partial \Phi_*}{\partial t} \sin k x \sin my \tag{7.17}$$

we find

$$\frac{\partial \Phi_*}{\partial t} = \frac{A}{p_o}\frac{f_o^2}{s^2}\left[\delta p_*^{\delta-1} - (\alpha+1)p_*^{\alpha}\right] \tag{7.18}$$

Figure 13 shows the geopotential tendency for the two cases: L = 1000km and L = 10000 km using the same values for the other parameters as before. The tendency is expressed in the unit: $mday^{-1}$.

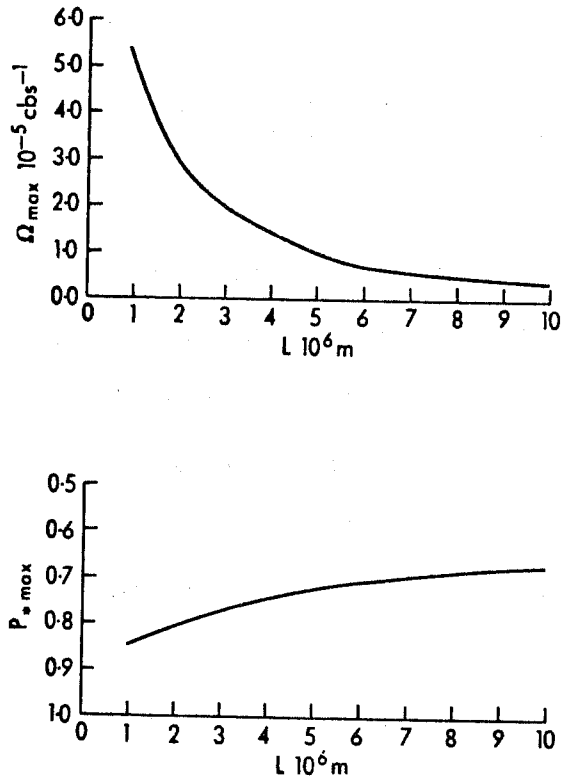

Fig.12: Upper part: The maximum value of - Ω as a function of wavelength. Parameters: $\sigma_o = 2$, $\alpha = 3$, $H_o = 10^{-1}$. All values in MTS-units.
Lower part: The values of normalized pressure at which - Ω has its maximum as a function of wavelength. Same parameters as above.

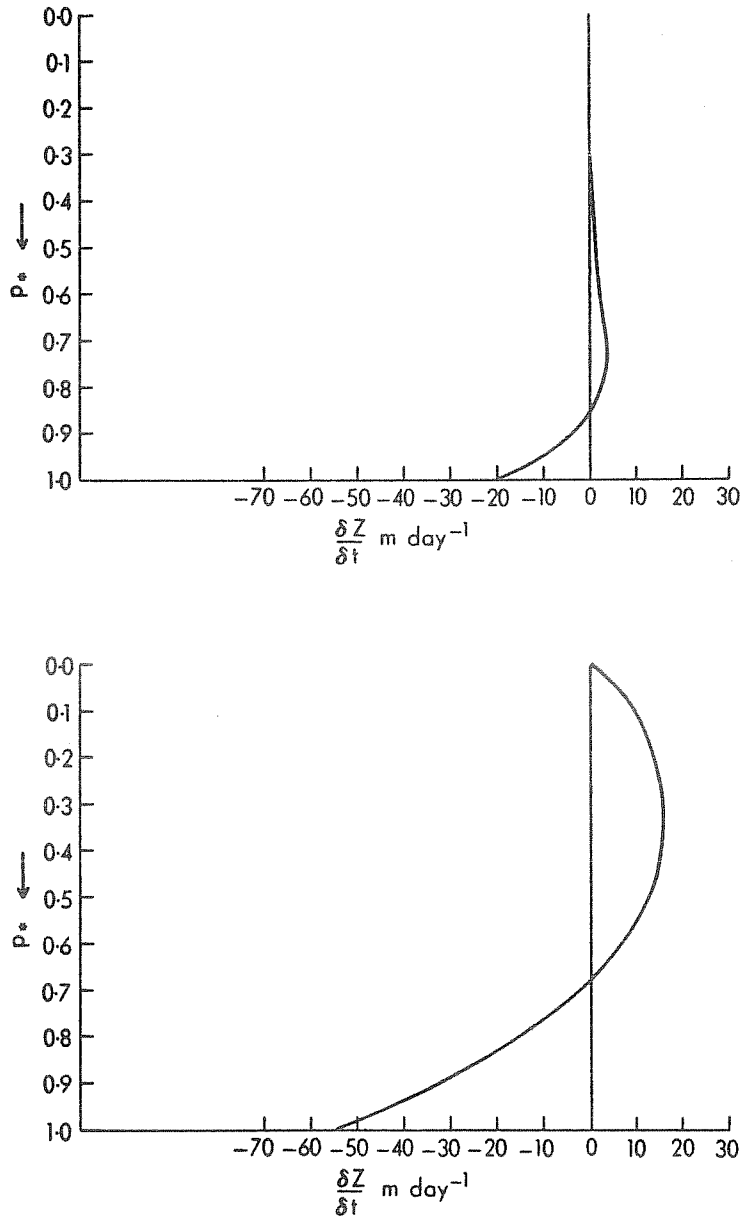

Fig.13: The geopotential tendency in $mday^{-1}$ as a function of normalized pressure. Parameters: $\alpha = 3, \sigma_o = 2$, $H_o = 10^{-1}$, $L = 10^6$ (upper part), $L = 10^7$ (lower part).

It is seen that the larger values of the geopotential tendency are obtained for the larger horizontal wavelength. This is due to the factor s^2 which appears in the denominator in (7.18). This scale dependence can be further illustrated by calculating the surface pressure tendency which is obtained by setting $p_* = 1$ in (7.18) and converting $\partial \Phi_*/\partial t$ to a pressure tendency using the hydrostatic equation. Figure 14 shows the surface pressure tendency, expressed in mb/3 hours, as a function of wavelength. The fall in the surface pressure generated by the heating increases with increasing wavelength.

The results quoted above are naturally determined by the specific specification of the heating, eq. (7.3), and the static stability, eq. (7.6), used in the calculations. It is of some interest to investigate how sensitive the results are to these specifications. For this purpose we shall give a couple of additional examples. The first example is one in which the static stability parameter is assumed to be constant replacing (7.6). Setting $\sigma=\bar{\sigma}=$ const. we must now solve (7.5). The solution is of the form

$$\Omega = \Omega_o(p_*) + C_1 e^{qp_*} + C_2 e^{-qp_*} \tag{7.19}$$

where

$$q = \left[\frac{\bar{\sigma} p_s^2}{f_o^2} (k^2+m^2)\right]^{\frac{1}{2}} \tag{7.20}$$

and where $\Omega_o(p_*)$ is a solution to (7.5).

$\Omega_o(p_*)$ is particularly simple to evaluate in the case where $\alpha = 2$ in which case we find

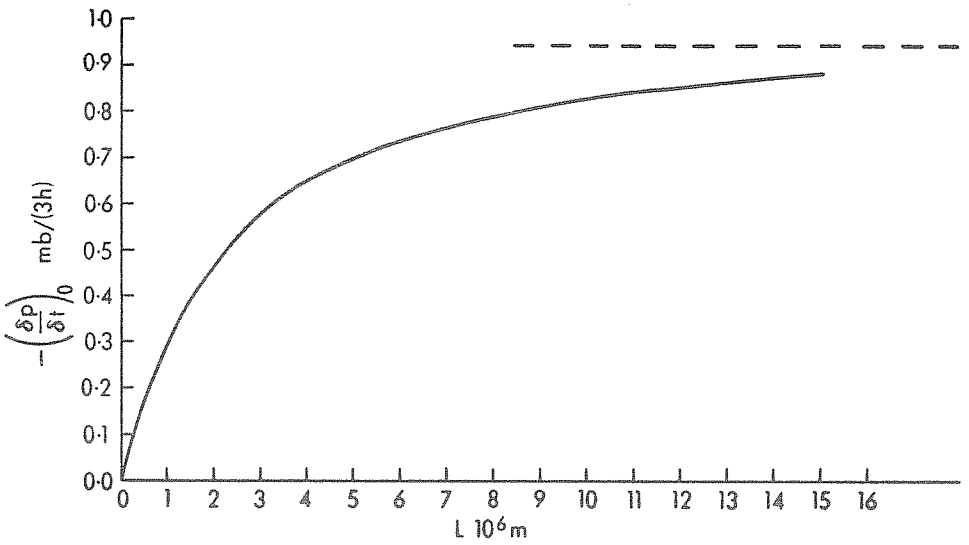

Fig.14: The negative value of the surface pressure tendency in mb/3 hours as a function of wavelength. Parameters: $\alpha = 3$, $\sigma_o = 2$, $H_o = 10^{-1}$.

$$\Omega_o(p_*) = -\frac{R}{C_p}\frac{H_o}{\sigma p_o}p_* = Bp_* \tag{7.21}$$

where

$$B \quad -\frac{R}{C_p}\frac{H_o}{\sigma p_o} \tag{7.22}$$

The integration constants in (7.19) are determined from the boundary conditions. From $\Omega = 0$, $p_* = 0$ we find $C_1 = -C_2$, and (7.19) can be written in the form

$$\Omega = Bp_* + C\sinh(qp_*) \tag{7.23}$$

From the condition $\Omega = 0$, $p_* = 1$ we find that

$$C = \frac{B}{\sinh(q)} \tag{7.24}$$

giving the final form

$$\Omega = \frac{R}{C_p}\frac{H_o}{\sigma p_o}\left(\frac{\sinh(qp_*)}{\sinh(q)} - p_*\right) \tag{7.25}$$

(7.25) must naturally be compared with the solution (7.8) for $\alpha=2$. We find in that case:

$$\Omega = \frac{R}{C_p}\frac{H_o}{p_o}\frac{s^2}{\frac{f_o^2}{6p_o^2} - \sigma_o s^2}(p_*^3 - p_*^\delta) \tag{7.26}$$

Figure 15 shows the comparisons between (7.25) and (7.26) for L = 1000km and L = 10000 km. In both cases we have used $H_o = 10^{-1}\text{kj}\ t^{-1}\text{sec}^{-1}$, $\sigma_o = 2$ and $\bar{\sigma} = 8$. It is seen that the formula with a constant static stability produces a smaller vertical velocity in the lower layers of the model atmosphere and a larger vertical velocity in the upper layers. This difference is particularly pronounced in the case of L = 1000 km.

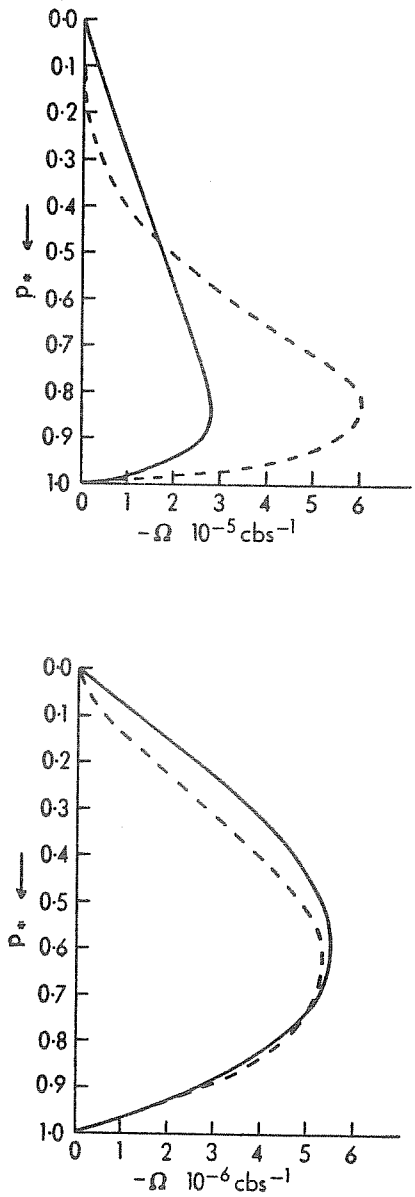

Fig.15: $-\Omega$ as a function of normalized pressure. Solid curve for a constant static stability ($\bar{\sigma} = 8$), dashed curve for a static stability which is inversely proportional to pressure. Parameters: $\alpha = 2$, $\sigma_o = 2$, $H_o = 10^{-1}$, $L = 10^6$ (upper part), $L = 10^7$ (lower part).

For each of the two cases it is naturally also possible to calculate the tendency in the geopotential as was done in (7.18). Figure 16 shows the comparison between the geopotential tendency in the two cases for L = 1000km and L = 10000km. The major difference is that in the previous case we had $\partial z/\partial t = 0$ for $p_* = 0$ while this relations is not satisfied in the new case. However, in the lower parts of the atmosphere there is good agreement between the two cases, especially for the larger value of the horizontal scale.

Figure 17 shows finally the pressure tendency for the case $\sigma=\bar{\sigma}=$ const. and $\alpha = 2$ as a function of wavelength. The curves are quite similar to those reproduced in Figure 14, especially for the larger values of L. For the smaller scale we find that the new case produces somewhat smaller values of $\left(\partial p/\partial t\right)_o$ in agreement with Figure 16.

The second special case is one in which we shall maintain (7.6) for the variation of $\bar{\sigma}$, but the vertical variation of the heating will be changed. Let us assume that the heating is constant, say $H = H_o$, in the interval $a \leq p_* \leq 1$, but zero for $0 \leq p_* < a$. (7.7) is now changed to

$$\frac{d^2\Omega}{dp_*^2} - \frac{\sigma_o p_o^2}{f_o^2}(k^2+m^2)\frac{\Omega}{p_*^2} = \frac{R}{C_p}\frac{H_o p_o}{f_o^2}(k^2+m^2)\frac{1}{p_*} \qquad (7.27)$$

for $a \leq p_* \leq 1$, while the right hand side of (7.27) is zero for $0 \leq p_* < a$.

For $0 \leq p_* < a$ we find the solution

$$\Omega = C_1 p_*^{\delta_1} \qquad (7.28)$$

satisfying the boundary condition at $p_* = 0$. In the remaining

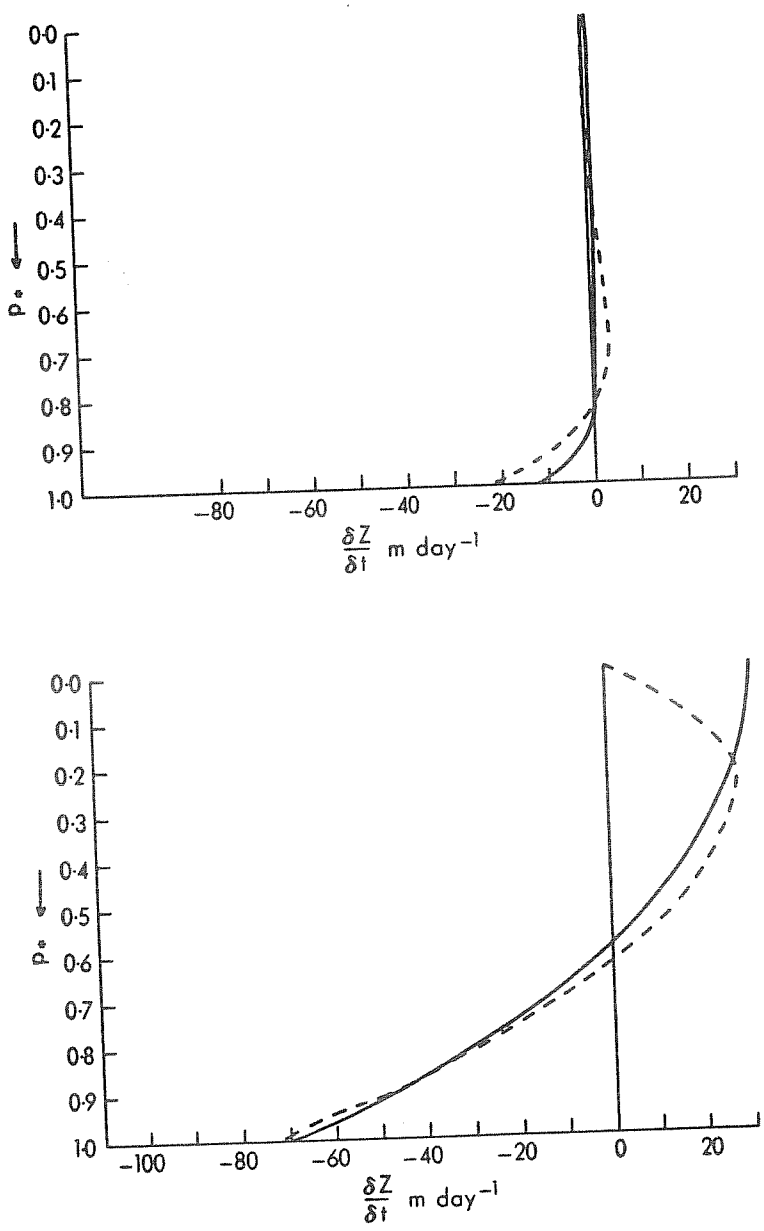

Fig.16: The geopotential tendency as a function of normalized pressure. Solid curve for a constant state stability ($\bar{\sigma}$ = 8), dashed curve for a static stability which is inversely proportional to pressure.
Parameters as in fig.15.

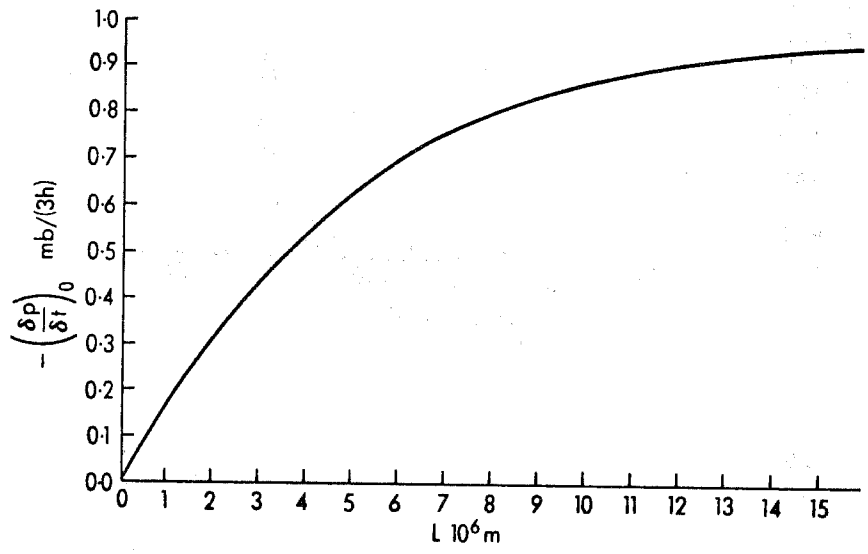

Fig.17: The negative value of the surface pressure tendency in mb/3 hrs as a function of wavelength.
Parameters: $\alpha = 2$, $\bar{\sigma} = 8$, $H_o = 10^{-1}$.

part of the atmosphere $a \leq p_* \leq 1$ we have

$$\Omega = Bp_* + C_2\, p_*^{\delta_1} + C_3\, p_*^{\delta_2} \tag{7.29}$$

where B is given in (7.22) and $\delta_1 = \delta$ in (7.9). δ_2 is obtained from (7.9) by a change of sign in front of the square root. The boundary condition at $p_* = 1$ results in

$$C_3 = -B - C_2 \tag{7.30}$$

In order to determine C_1 and C_2 we shall employ the requirements that Ω and $d\Omega/dp_*$ are continuous at $p_* = a$. The two conditions lead to linear equations from which C_1 and C_2 can be determined. We note the results:

$$C_1 = B\left\{\frac{\delta_1 - 1}{\delta_1 - \delta_2}\, a^{1-\delta_2} + \frac{1-\delta_2}{\delta_1 - \delta_2}\, a^{1-\delta_1} - 1\right\} \tag{7.31}$$

and

$$C_2 = B\left\{\frac{\delta_1 - 1}{\delta_1 - \delta_2}\, a^{1-\delta_2} - 1\right\} \tag{7.32}$$

The solutions for Ω are therefore

$$\Omega = B\left\{\frac{\delta_1 - 1}{\delta_1 - \delta_2}\, a^{1-\delta_2} + \frac{1-\delta_2}{\delta_1 - \delta_2}\, a^{1-\delta_1} - 1\right\} p_*^{\delta_1}; \quad 0 \leq p_* < a \tag{7.33}$$

and

$$\Omega = B\left\{(p_* - p_*^{\delta_2}) + \left(\frac{\delta_1 - 1}{\delta_2 - \delta_1}\, a^{1-\delta_2} - 1\right)(p_*^{\delta_1} - p_*^{\delta_2})\right\}; \quad a \leq p_* \leq 1 \tag{7.34}$$

The distributions of Ω according to (7.33) and (7.34) are shown in Figure 18 which was constructed using the following parameters:

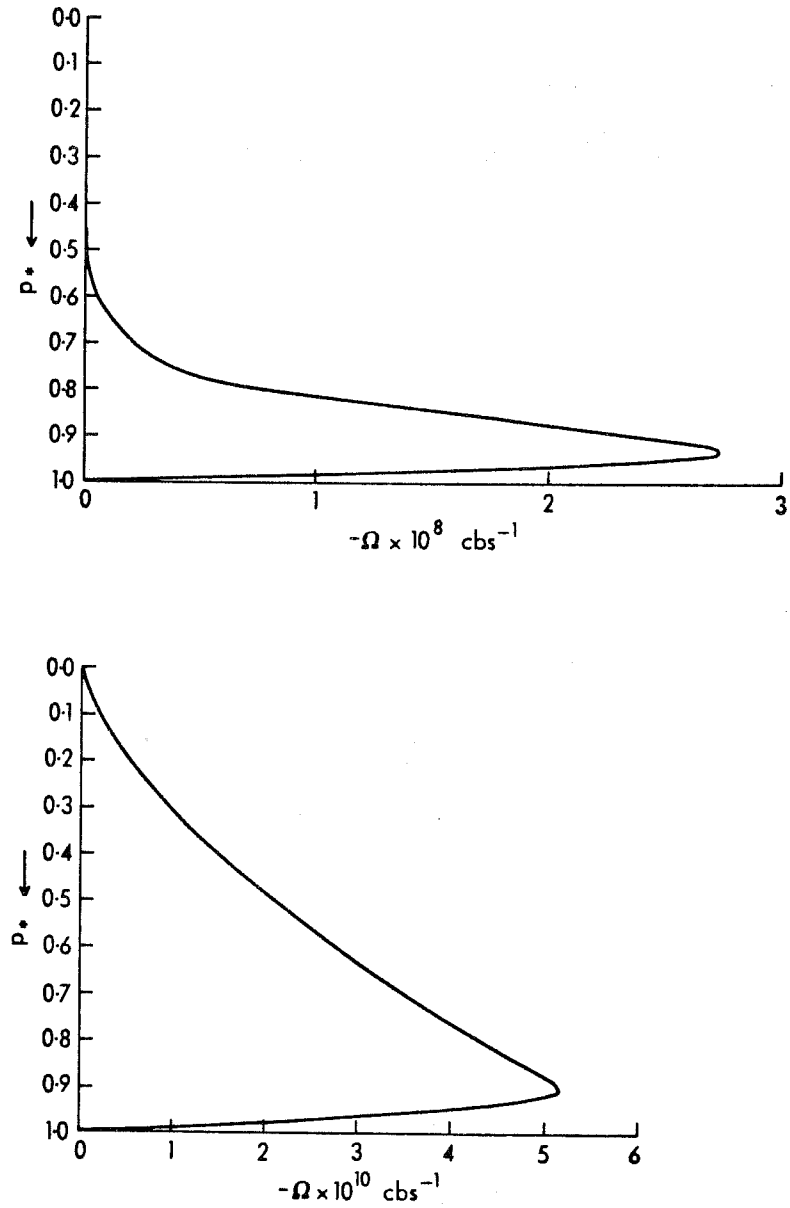

Fig.18: $-\Omega$ as a function of normalized pressure for the case in which the heating is constant in the lowest 10cb layer and zero in the rest of the atmosphere. Parameters: $\sigma_o = 2$, $a = 0.9$, $H_o = 10^{-1}$, $L = 10^6$ (upper part), $L = 10^7$ (lower part).

$H_o = 10^{-1}$kj t^{-1}sec^{-1}, a = 0.9 and L = 1000km and 100000km, respectively. The value of a indicates that only the lowest 10 cb of the atmosphere is being heated. As with the earlier examples it is found that the general magnitude of Ω is larger for the small value of L than for the large value. Secondly, for the small value of L we find that the signficant values of Ω are found in the lower layers of the atmosphere, while L = 10000 km produces non-zero values of Ω quite high up in the model. The maximum value of $-\Omega$ is in each case found near the top of the heated layer, i.e. at $p_* = 0.93$ for L = 1000km and at $p_* = 0.91$ for L = 10000km. Note also that the vertical velocities in Figure 18 are smaller in absolute values than the corresponding values in Figures 11 and 15. This relationship is supposedly due to the fact that the heating is concentrated in a more shallow layer (10 cb) as compared to heating the total column. In the former case we find that the total heating for the atmospheric column is $(poHo)/g(\alpha+1)$ which for $\alpha = 3$ gives 0.34 kj sec^{-1}, while the latter case gives $(\Delta p)H_o/g = 0.1$ kjsec^{-1}.

We shall next explore the pressure changes produced at the surface by the heating. Following the procedure outlined in (7.17) and (7.18) we find that

$$\left(\frac{\partial Z}{\partial t}\right)_{p_*=1} = -\frac{f_o^2}{s^2}\ \frac{B}{p_o g}\ \left\{(1-\delta_2)+(\delta_1-1)a^{1-\delta_2}-(\delta_1-\delta_2)\right\} \qquad (7.35)$$

Converting (7.35) into the pressure tendency at the surface we find

$$\left(\frac{\partial ps}{\partial t}\right) = -\frac{f_o^2}{s^2}\ \frac{B}{RT_o}\ (\delta_1-1)\left[a^{1-\delta_2}-1\right] \qquad (7.36)$$

In order to further evaluate (7,36) we make use of the fact that $\delta_1 + \delta_2 = 1$ and

$$s^2 = \frac{f_o^2}{\sigma_o p_{o2}} \delta_1(\delta_1-1) \tag{7.37}$$

where the last equation is obtained from (7.9). Introducing the expression for B and (7.37) in (7.36) we find

$$(\frac{\partial ps}{\partial t}) = - \frac{H_o p_o}{C_p T_o} \frac{1-a^\delta}{\delta} \tag{7.38}$$

The limiting value of $\partial ps/\partial t$ for $L \to \infty$ is found by setting $\delta = 1$, and we get

$$\lim_{L\to\infty} (\frac{\partial ps}{\partial t}) = - \frac{H_o p_o}{C_p T_o} (1-a) \tag{7.39}$$

Using the values adopted earlier ($H_o = 10^{-1} kjt^{-1} sec^{-1}$, $p_o = 100cb$, $C_p = 1004\ m^2 sec^{-2} deg^{-1}$ and $T_o = 288^oK$, $a = 0.9$) we find that $\partial ps/\partial t$ in the limit is 0.38 mb/3 hrs. On the other hand if the heating had been constant through the column up to a = 0.1 we would find a limiting pressure change of 3.4 mb/3 hrs. Figure 19 shows ($\partial ps/\partial t$) as a function of the horizontal scale.

The examples in this section indicate clearly the main meachanisms of diabatic heating and its influence on the vertical velocity, the changes of the geopotential and the surface pressure. The modifying influence of the heating on the development of atmospheric systems is clearly indicated in spite of the schematic specifications of heating and static stability.

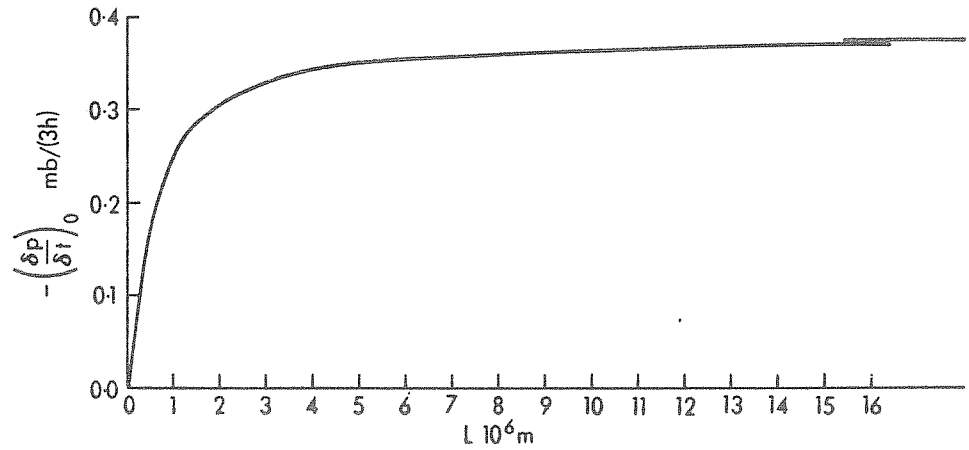

Fig.19: The negative value of the surface pressure tendency in mb/3 hrs as a function of wavelength for the case and the parameters given in Fig.18.

8. Concluding Remarks.

The investigation has first of all given insight into the influence of Newtonian heating on the speed of propagation and the growth of atmospheric waves. The simplified form of the heating considered in Sections 2, 3, 4 and 5 results in general in a damping of the atmospheric waves accompanied by a destruction of available potential energy and a conversion from kinetic to available potential energy. When the basic state has a vertical windshear we find that the Newtonian heating creates instability for all scales larger than a certain critical scale, but outside the region of instability in the adiabatic case it is found that the e-folding times are quite large. The general result inside the region of instability in the adiabatic case is that the Newtonian heating increases the e-folding times.

Another effect of the Newtonian heating is that the Rossby type waves will be damped with rather small values of the e-damping times. Based upon the perturbation analysis it would appear that the very long waves in the atmosphere are not Rossby waves, but rather of the internal type which move much more slowly from east to west relative to the basic current.

The tendency calculations presented in section 7 show the order of magnitude of the influence of the heating on the geopotential, the surface pressure and the vertical velocity. In addition, the importance of the vertical variation of the heating has been investigated.

REFERENCES

Döös, B.R., 1961: The scale of non-adiabatic heating as a factor in cyclogenesis, Journal of Meteorology, Vol.18, pp. 1-8.

Döös, B.R., 1969: The influence of the large-scale heat sources on the dynamics of the ultra-long waves, Tellus, Vol.21, pp. 25-39.

Fisher, P. and A. Wiin-Nielsen, 1971: On baroclinic instability of ultra-long waves, Tellus, Vol.23, pp. 269-284.

Gates, W.L., 1961: Static stability measures in the atmosphere, Journal of Meteorology, Vol.18, pp. 526-533.

Haltiner, G.J., 1967: The effects of sensible heat exchange on the dynamics of baroclinic waves, Tellus, Vol.19, pp. 183-198.

Jacobs, S.J. and A. Wiin-Nielsen, 1966: On the stability of a barotropic basic flow in a stratified atmosphere, Journal of Atmospheric Science, Vol.23, pp. 682-687.

Petterssen, S., 1950: Some aspects of the general circulation of the atmsophere, Centenary Proceedings, Royal Meteorological Society, pp. 120-155.

Petterssen, S., 1955: A general survey of factors influencing developments at sea level, Journal of Meteorology, Vol.12, pp. 36-42.

Wiin-Nielsen, A., 1959: On barotropic and baroclinic models with special emphasis on ultra-long waves, Monthly Weather Review, Vol. 87, pp.171-183.

Wiin-Nielsen, A, 1961: A preliminary study of the dynamics of transient, planetary waves in the atmosphere, Tellus, Vol.13, pp. 320-333.

Wiin-Nielsen, A., 1971: On the motion of various vertical modes of transient very long waves, part I, Tellus, Vol.23, pp. 87-98.

Wiin-Nielsen, A., 1972: As above, part II, Tellus, Vol.23, pp. 207-217.

Wiin-Nielsen, A., 1972: Simulations of the annual variation of the zonally-averaged state of the atmosphere, Geofysiske Publikasjoner, Vol.28, No.6, pp. 1-45.

Wiin-Nielsen, A., A.Vernekar and C.H.Yang, 1967: On the development of baroclinic waves influenced by friction and heating, Pure and Applied Geophysics, Vol.68, pp. 131-161.

Winston, J.S., 1955: Physical aspects of rapid cyclogenesis in the Gulf of Alaska, Tellus, Vol.7, pp. 481-500.